R. & M. No. 3100
(19,451)
A.R.C. Technical Report

MINISTRY OF SUPPLY

AERONAUTICAL RESEARCH COUNCIL
REPORTS AND MEMORANDA

Experiments with a Two-Dimensional Aerofoil Designed to be Free from Turbulent Boundary-Layer Separation at small Angles of Incidence for all Mach Numbers

By

D. W. Holder, D.Sc., and R. F. Cash
of the Aerodynamics Division, N.P.L.

LONDON: HER MAJESTY'S STATIONERY OFFICE
1959
PRICE 17*s*. 6*d*. NET

Experiments with a Two-Dimensional Aerofoil Designed to be Free from Turbulent Boundary-Layer Separation at small Angles of Incidence for all Mach Numbers

By

D. W. Holder, D.Sc., and R. F. Cash
of the Aerodynamics Division, N.P.L.

Communicated by the Director-General of Scientific Research (Air),
Ministry of Supply

Reports and Memoranda No. 3100*
August, 1957

Summary.—The present investigation was designed primarily to check the validity of a simple method which had been suggested for designing an aerofoil section on which, for a limited range of incidence, turbulent boundary-layer separation is absent at all values of the free-stream Mach number. Assuming that this method proved successful, a second object was to study the transonic flow past the aerofoil, and to compare the results with previous speculations concerning the nature of the flow when separation is absent. Since separation was expected to occur when the angle of incidence was increased to a sufficiently large value, a third object was to study the flow when separation was present and, in particular, to confirm whether the effects of separation are less severe for the present section than for most previous sections.

The method of designing the section to avoid separation involved the use of a small trailing-edge angle, the value being determined by the incidence range over which separation is required to be absent. The trailing-edge angle was chosen to be 3 deg, and this was achieved on a 4 per cent thick symmetrical section without concave curvature by using a well-forward (0·2 chord) position of maximum thickness. This section was expected to give flow free from shock-induced separation at angles of incidence less than $1\frac{1}{2}$ deg, and this expectation was realized in the experiment.

In general, the study of the flow past the aerofoil when separation was absent substantiated previous conjectures concerning its major features. In particular, it was found that, when the free-stream Mach number was raised, the shock wave on the upper surface moved back to the trailing edge before that on the lower surface. This behaviour is in contrast to that observed on previously tested sections, where the effects of separation have resulted in the lower-surface shock reaching the trailing edge first with, in most cases, undesirable effects on the loading on the section. However, it was found that the boundary layer, although not separating, evidently still had significant effects on the flow, and it is considered that a full understanding must await further research, notably on the pressure distribution through a weak normal shock interacting with a flat-plate boundary layer, and on the pressure changes along wakes.

The third object of the experiment, namely, to investigate whether, when boundary-layer separation occurred, the effects were less severe on the present section than on most previous sections, was also generally successful. Thus, when the free-stream Mach number was raised at a fixed angle of incidence, it was found that the upper-surface shock wave moved aft relatively smoothly even when severe separation occurred at the shock. This result is attributed to the fact that the section shape is such that the local Mach number ahead of the shock does not change greatly as the shock moves aft, so that the locus of the pressure behind the shock is relatively uniform along the chord instead of falling rapidly when the shock has, in its rearwards movement, become strong enough to provoke separation. In other words the nature of the flow pattern behind the shock does not change greatly as the shock moves aft, and it is envisaged that the pressure distribution behind the shock moves, as it were, downstream with the shock and into the wake without substantial change.

* Published with the permission of the Director, National Physical Laboratory.

Another feature of the results obtained at large angles of incidence is that the flow on the major part of the lower surface appears to be relatively independent of disturbances to the trailing-edge pressure produced by the effects of flow separation on the upper surface. This result arises because, when the aerofoil is at a sufficiently large incidence for the lower surface to be inclined downwards at the trailing edge with respect to the free stream, there is a rapid acceleration along the lower surface just ahead of the trailing edge. The effects of disturbances to the trailing-edge pressure appear to be largely confined to this region of local acceleration, and to become relatively small further forward on the lower surface. Also, because of the acceleration near the trailing edge, sonic flow occurs in this region at a comparatively low free-stream Mach number, and when this has happened the requirement that the static pressures near the trailing edge must be approximately equal on the two surfaces can be satisfied by local expansion and shock waves at the trailing edge, instead of by a general adjustment of the lower-surface flow.

At very large angles of incidence ($\alpha > 6$ deg), separation occurs at the leading edge for low Mach numbers, but the flow reattaches when the Mach number is raised. The resultant changes of pressure distribution are, in general, similar to those observed on other aerofoils.

The loading on the aerofoil varies with Mach number because of the changes in pressure distribution, but, since these changes occur more smoothly than on most aerofoil sections, the variations of loading do not take place so abruptly.

---

1. *Introduction.*—It is well known that the occurrence of boundary-layer separation at the shock waves that are present at high subsonic and transonic speeds may have undesirable effects on the characteristics of aerofoil sections. When attempting to reduce or eliminate these effects two approaches are possible. One is to use a method of boundary-layer control with the object of thinning or removing the boundary layer, or of modifying its profile so that it can withstand a greater pressure gradient before or after separating. The other approach is to design the section shape in such a way that the shock strength is minimized, or so that when separation occurs its effects on the flow pattern are small.

In the present investigation the second approach was followed, and the aerofoil section was so designed that, for a limited range of lift coefficient, the shock waves formed at any free-stream Mach number were expected to be too weak to provoke separation. Within this range of lift coefficient it was, therefore, hoped to study for the first time the transonic flow past an aerofoil when separation is entirely absent, and to compare the observations with the type of flow expected (*see*, for example, Refs. 1, 2 and 3). At larger lift coefficients separation was expected to occur, but it was hoped that the effects on the characteristics of the aerofoil would be reduced by certain features of the design (*i.e.*, the small trailing-edge angle, and the large extent of flat surface upstream of the trailing edge).

2. *The Method Used to Design the Aerofoil Section.*—If the angle of incidence is constant, the nearly normal shock formed near the surface of an aerofoil at high subsonic speeds moves rearwards when the free-stream Mach number is raised, as shown in the local Mach-number distributions sketched in Fig. 1. If the boundary layer is turbulent, it has been established[1, 2] that separation will occur at the shock when the local Mach number immediately upstream exceeds about 1·23 (depending to some extent on section shape and free-stream Mach number). Thus, separation would be expected to be absent if the section shape can be designed so that, for the particular value of the incidence, this value of the local Mach number is not reached ahead of the shock at any stage in its rearwards movement.

An approximate method for designing the section to achieve this result is suggested in Ref. 4. It is shown that for free-stream Mach numbers close to unity, where the shocks have moved back to the trailing edge and are inclined to the flow (Fig. 2), the local Mach number $M_{\text{T.E.}}$ ahead of the upper-surface* shock is simply related to the flow-deflection angle $\delta_{\text{T.E.}}$† at the trailing edge as shown in Fig. 3. This diagram is reproduced from Ref. 4, and is supported by additional results

---

* Since, for a symmetrical section, the local Mach numbers are larger on the upper than on the lower surface, the upper surfaces only need be considered in the present discussion.

† Assuming zero downwash, this is equal to the sum of the semi-trailing edge angle and the angle of incidence, for a symmetrical aerofoil.

obtained more recently including the results of the present experiment.* When Ref. 4 was written, data were available only for free-stream Mach numbers below unity, and it was accordingly assumed that the correlation shown in Fig. 3 (which implies that the local Mach number just downstream of the trailing edge is nearly constant) arose because the changes of displacement thickness along the wake were insensitive to the shape and incidence of the aerofoil. More recently, however, it has been found that the correlation also exists for free-stream Mach numbers slightly greater than unity. In this case the pressure distribution downstream of the aerofoil may be influenced by the incoming family of characteristics resulting from the reflection from the sonic line of expansion waves originating at the aerofoil. When the free-stream is supersonic it is, however, difficult to see how the conditions downstream of the trailing edge can affect the flow over the aerofoil, and, since this evidently adjusts itself to give the values of $M_{\text{T.E.}}$ shown in Fig. 3, there are at present uncertainties (*see* Ref. 13) about the fundamental mechanism involved.

If it is assumed that the effect of the incoming family of characteristics can be neglected as a first approximation (*i.e.*, the flow is a simple-wave flow), the Mach number $M_{\text{T.E.}}$ is, for a section without concave curvature, higher than the local Mach number reached at any point on th surface during the rearwards movement of the shock with increasing free-stream Mach number. Thus, if the value of $\delta_{\text{T.E.}}$ is sufficiently small for the value of $M_{\text{T.E.}}$ to be below about $1 \cdot 23$, shock-induced separation should be absent. According to Fig. 3, the corresponding value of $\delta_{\text{T.E.}}$ is about 3 deg, and the present aerofoil was designed with a semi-trailing-edge angle of $1 \cdot 5$ deg in order to give separation-free flow up to an angle of incidence of about $1 \cdot 5$ deg. Although shock-induced separation was expected when the angle of incidence exceeded $1 \cdot 5$ deg, no large effects on the overall flow pattern were anticipated until the region of separated flow became of large extent. On the basis of Ref. 2 it was considered that this would occur when the flow behind the shock wave first became sonic, which usually arises when the Mach number ahead of the shock rises to about $1 \cdot 27$. According to Fig. 3, the corresponding flow-deflection angle at the trailing edge is approximately 4 deg, so that appreciable separation effects were not expected until the incidence was increased to $2\frac{1}{2}$ deg.

When the free-stream Mach number is raised to a value appreciably in excess of unity, the above considerations cease to apply. Under these conditions the tendency for separation to occur ahead of the inclined trailing-edge shock is, however, much less severe than at the nearly normal shock present at high subsonic speeds. Thus an aerofoil section that is free from separation at high subsonic and transonic speeds would be expected to be free from separation at all values of the free-stream Mach number.

The argument outlined above enables the trailing-edge angle to be specified, but leaves the design of the remainder of the section to be decided. In practice this decision would depend to some extent on the plan-form of the wing, and on the range of Mach number over which it was to operate. For example, if the leading edge was supersonic at the top end of the speed range, a section with a sharp leading edge would probably be desirable for performance considerations, whereas if the leading edge was subsonic a section with a rounded leading edge might be preferable. If the maximum-thickness position is well aft, a very thin section is needed to provide the small trailing-edge angle (e.g., $t/c \simeq 1 \cdot 3$ per cent for a symmetrical biconvex section with a semi-trailing-edge angle of $1\frac{1}{2}$ deg) unless a blunt trailing edge is used. The use of such a thin section would have made the construction of the model difficult, and limited the range of lift coefficient over which it could be tested. On the other hand, the presence of a trailing edge of large thickness would have complicated the flow, and made it difficult to apply the results to the design of conventional sections. The use of negative camber reduces the flow-deflection angle at the trailing edge of the upper surface and, on the basis of the approach outlined above, would thus be expected to give a flow free from shock-induced separation for larger angles of incidence, although it is not clear whether the lift coefficient for the onset of separation would be increased.

* Because of the effects of the bluntness of the trailing edge, the values plotted in Fig. 3 are obtained by extrapolating to the trailing edge the pressures measured further forward on the aerofoil surface.

In addition to the problem of avoiding separation at low incidence, the question of reducing the effects of separation at large angles of incidence was considered. Here there was some evidence[2] that a large extent of flat surface ahead of the trailing edge was beneficial, since this reduces the increase of local Mach number ahead of the shock when the shock moves aft, and hence the associated development of the separated flow. Accordingly it was decided to use a symmetrical aerofoil of moderate thickness ratio (4 per cent), and to achieve the small trailing-edge angle by employing a well-forward position of maximum thickness (20 per cent chord) giving an almost straight-sided section over a large part of the chord ahead of the trailing edge. The forward position of maximum thickness also enabled a leading-edge radius to be used which was relatively large for a section of this thickness ratio, thus delaying the onset of leading-edge separation at low speeds.

To facilitate calculations made for comparison with the experimental results, the section* was designed on the basis of an analytical formula[6], the x and y co-ordinates (Fig. 4a) being related by the expression

$$y = (c' - x)[1 - \{(c' + s)(c' - x)\}^n \tanh \sqrt{\left[2\left\{\left(\frac{x + s}{s}\right)^2 - 1\right\}\right]} \tan \frac{\tau}{2}, \qquad .. \qquad (1)$$

where τ is the trailing-edge angle, n is a constant put equal to 9 for the present section, and c' and s are lengths chosen as 9·409 in. and 0·341 in. respectively for the present section. The chord of an aerofoil whose co-ordinates satisfy equation (1) is equal to c' if the trailing-edge thickness is zero, but for structural reasons the actual chord c of the present aerofoil was made equal to 9 in. by cutting off the trailing edge so that its thickness was 0·02 in. The co-ordinates of the section are set out in Table 1, and the positions of the pressure tappings in the surface are given in Table 2. The section shape is drawn in Fig. 4a; it is free from discontinuities in slope and curvature, and, as seen in Fig. 4b, the upper and lower surfaces are almost flat between about 0·3 chord and the trailing edge.

The theoretical pressure distribution at zero incidence was calculated[7] by the method of Ref. 8 for incompressible flow, and by the method of Ref. 9 for a Mach number M_0, of 0·70. The results are plotted in Fig. 5 which also includes the measured values at $M_0 = 0{\cdot}70$, and shows that these are in good agreement with the results of the calculations except very close to the trailing edge. Here the slight trailing-edge bluntness (0·002 chord or approximately 0·05 of the boundary-layer thickness at the trailing edge), together with the effect of the boundary-layer growth along the surface, lead to pressures which are appreciably below those predicted on the assumption that the trailing edge is sharp (*see* also Section 10). It is seen in Fig. 5 that at zero incidence there is a suction peak at about 0·1 chord, and that downstream the pressure rises at a decreasing rate, the pressure gradient becoming approximately constant over the nearly flat part of the surface.

3. *Experimental Details.*—The aerofoil spanned the 14 in. width of the N.P.L. 36 in. × 14 in. High-Speed Wind Tunnel, and was supported by tongues passing through slots cut in the optical glass windows fitted in the side walls of the tunnel. The pressure leads to the manometer were carried out of the tunnel through the tongues. The tunnel was fitted with slotted walls for subsonic and transonic operation, and with solid nozzle-shaped walls when used at supersonic speeds. The solid blockage of the aerofoil was about 1 per cent; no corrections were applied for boundary interference, and the values of the free-stream Mach number quoted are, therefore, inaccurate especially for Mach numbers close to unity.

Since the tunnel operates at constant (approximately atmospheric) stagnation pressure, the Reynolds number varies when the Mach number is changed, typical values (based on chord) being $1{\cdot}9 \times 10^6$ at $M_0 = 0{\cdot}4$, $3{\cdot}6 \times 10^6$ at $M_0 = 1{\cdot}0$, and $3{\cdot}5 \times 10^6$ at $M_0 = 1{\cdot}6$. At these Reynolds numbers it was found that, when transition was free, the boundary layer remained laminar back to the trailing edge at low Mach numbers in spite of the adverse pressure gradients shown in Fig. 5,

* In the list of aerofoil sections designed at the N.P.L.[5], the section is referred to as NPL 491.

and to the shock waves at higher Mach numbers. In order to make the results applicable to full-scale conditions (*see*, for example, Ref. 10), transition to turbulent flow was fixed artificially by means of carborundum grains cemented uniformly over the first 0·05 chord of both the upper and lower surfaces of the aerofoil.

Schlieren and direct-shadow photographs* were taken for each value of the angle of incidence and Mach number, and the examples reproduced in Figs. 24 to 27 are discussed below in connection with Fig. 22. The photographs were used to determine the shock-wave position, and this information was used in drawing the surface-pressure distributions through the limited number of measured points. The photographs were also used to detect the presence and position of boundary-layer separation and, in some cases, to estimate the position of flow reattachment.

4. *Experimental Results.*—The static-pressure distributions over the upper and lower surfaces of the aerofoil are shown in Figs. 6 to 17 for a range of angles of incidence and free-stream Mach numbers, and the integrated lift and quarter-chord pitching-moment coefficients, and centre-of-pressure positions are plotted in Figs. 18 to 20. The form-drag coefficients for a limited range of incidence are reproduced in Fig. 21.

Before discussing these results in detail, it is convenient to consider briefly the types of flow that were observed at various values of the Mach number and angle of incidence. As anticipated, it was found that, under certain conditions, boundary-layer separation was absent at all values of the Mach number. These conditions are displayed in Fig. 22, which shows boundaries (plotted on an angle-of-incidence, Mach-number basis), dividing the regimes of flow in which separation was absent from those in which separation occurred at the leading edge and at a shock wave. The approximate conditions for which the shock waves were nearly normal, and for which inclined shocks existed at the trailing edge are indicated. When, at supersonic speeds, there were inclined shocks at the trailing edge, the angle of incidence could not for structural reasons be raised to a value for which separation occurred. Accordingly, the boundary in Fig. 22 has, for this type of flow, been drawn at the value found in previous experiments on boundary-layer separation in supersonic flow[11, 12]. The conditions for the first occurrence of sonic flow and the first appearance† of shock waves are shown in Fig. 23. This also includes the conditions for which the shock waves first reach the trailing edge, and for which sonic flow first occurs there; the boundary for the ' divergence ' of the trailing-edge pressure (*see* Section 12) is also shown.

Schlieren photographs illustrating the different régimes of flow, and the way in which the régime changes when the Mach number or angle of incidence is altered are reproduced in Figs. 24 to 27.

For small angles of incidence ($\alpha < 1\frac{1}{2}$ deg), separation does not occur at any Mach number, and the development of the flow pattern with increasing Mach number is then as shown in Fig. 24. For moderate values ($1\frac{1}{2}$ deg $< \alpha < 6$ deg) separation is absent at low Mach numbers, but occurs at the shock wave when the Mach number is raised as shown in Fig. 25. Shock-induced separation then persists as the shock wave moves rearwards with increasing Mach number, until a value is reached when the shock waves are at the trailing edge, and are inclined to the flow. Separation is then absent, and remains so with further increase of Mach number.

When the incidence is increased at low Mach number, leading-edge separation occurs when $\alpha \doteq 6$ deg as shown in Fig. 26. If, however, the Mach number is raised at a large angle of incidence, the flow reattaches to the leading edge as shown in Fig. 27, and shock-induced separation occurs further aft on the upper surface.

---

* In some of the photographs a white line is visible running parallel to the rear of the upper surface. This occurs because the aerofoil bends slightly when the loading is large, so that light rays, entering the working-section parallel to the undistorted span, are reflected from the surface.

† Since the determination of the conditions for the first appearance of shock waves is to some extent dependent on the sensivity of the schlieren apparatus, and the interpretation of the photographs, the curves in Fig. 23 should be regarded as approximate.

5. *Discussion of the Results.*—The results outlined in the previous section will now be discussed in detail on the lines indicated below.

5.1. *Method of Analysis.*—When analysing the results obtained from experiments on aerofoils at high subsonic speeds it has proved useful[1,2] to consider separately for each surface the flow between the leading edge and the shock, near the shock, and between the shock and a point far downstream. Referring to Fig. 28, the static pressure p_1 at the surface just ahead of the shock follows a certain locus (*see* Section 6) as the shock moves rearwards over the aerofoil. This p_1 locus is frequently close to the ' sonic-range ' pressure distribution obtained at Mach numbers close to unity when the shock has moved back to the trailing edge, and is determined by the position of the sonic point on the surface and the geometry of the surface and of the sonic line. Of the factors considered here as determining the flow round the section at high subsonic speeds, the p_1 locus is probably the only one not critically dependent on viscous effects. When the shock moves rearwards, the static pressure p_2 just downstream also follows a locus (*see* Section 7) which is related to the p_1 locus by the pressure rise across the shock.

The free-stream static pressure p_0 is reached at infinity downstream, and is related to p_2 by the pressure changes between the shock and a point far behind the trailing edge. For a particular free-stream pressure, the shock position on each surface of the aerofoil is, therefore, considered as being determined by the intersection (*see* Fig. 28) of the p_2 locus with the curve of downstream pressure variation passing through the value of p_0 under consideration. On passing upstream through the shock, the pressure falls to approximately* the value of p_1 for the same chordwise position, and ahead of the shock the pressure distribution is similar† to the p_1 locus.

Part of the pressure change between the shock and a point far downstream occurs along the surface between the shock and the trailing edge, and part occurs along the wake. Although the division is rather artificial, it is convenient to consider the pressure changes in these two regions separately for the following reasons. Firstly, no measurements were made of the pressure distribution along the wake, so that the pressure changes there are a matter for conjecture, whereas those over the rear of the section may be discussed with greater confidence on the basis of the experimental observations. Secondly, the wake can support no appreciably transverse pressure gradient, so that the pressure distribution along the wake must be nearly the same on the upper and lower surfaces. The curves of pressure change between the shocks on the two surfaces and the free-stream pressure must, therefore, become approximately identical downstream of the trailing edge as sketched in Fig. 28. As a result, (*see* below), the value of the trailing-edge pressure plays an important part in relating the flows on the upper and lower surfaces, and it is convenient to use it in the analysis.

The pressure change along the wake will depend on the inviscid-flow pressure distribution downstream of the trailing edge, and on the effects of the boundary layers shed from the aerofoil. If attention is confined to small ranges of Mach number and lift coefficient, and to a region fairly close to the trailing edge, the effects of the boundary layers have been found in previous work to be very important. If, as a result of boundary-layer thickening or separation on one surface, the boundary layer at the trailing edge on that surface is affected, the pressure distribution along the wake will change. For a given free-stream Mach number (*i.e.*, value of p_0), it follows that the pressure just downstream of the trailing edge will also change. If the flow at the trailing edge is subsonic, and the trailing edge is sharp, this pressure will be closely equal to the pressures on the upper and lower surfaces just ahead of the trailing edge.

Thus, if the boundary layer on the upper surface thickens or separates at the shock wave, it will alter the shock position for a given free-stream pressure, partly because it will affect the pressure rise through the shock and hence the p_2 locus, and partly because it will affect the curve

* Since the pressure at the surface does not change abruptly through the shock, the curve representing the pressure change through the shock actually meets the p_1 and p_2 loci at somewhat different chordwise positions.

† For the reasons discussed in Section 8, the p_1 locus does not coincide with the sonic-range distribution nor with the pressure distribution ahead of the shock at lower Mach numbers.

of pressure change between the shock and a point far downstream. So long as the effects of boundary-layer thickening on the downstream pressure change are confined to the region between the shock and the trailing edge, their influence will be largely confined to the flow over the upper surface. When, however, the effect on the upper-surface pressure distribution extends to the trailing edge, the pressure distribution along the wake and hence the pressure at the rear of the lower surface will be affected, and the flow (*e.g.*, the shock position) on the lower surface will change in order to satisfy this modification of the trailing-edge pressure. This change in the lower-surface flow may in some cases result in a change in the thickness or profile of the boundary layer shed from the lower surface, which will in turn (together with the small changes in the inviscid flow resulting from the modification to the lower-surface flow), alter the pressure distribution along the wake, and hence the shock position on both surfaces. When, therefore, the flow in the wake is disturbed as a result of boundary-layer thickening or separation on one surface of an aerofoil, it is envisaged that the whole flow pattern adjusts itself until the flow over each surface again gives equal static pressures near the trailing edge, the value of this pressure being related to the free-stream pressure by the (modified) pressure change along the wake.

The ideas discussed above have proved of considerable value (*see*, for example, Refs. 1, 2 and 3) in analysing the effects of shock-induced and leading-edge separation on the flow past aerofoils, and in the following Sections of the paper they will be used as a framework for discussing the results of the present investigation.

6. *The Static Pressure p_1 at the Surface Immediately Upstream of the Shock on the Upper Surface.*—As discussed in the previous Section, the static pressure p_1 just ahead of the shock wave follows a certain locus (shown by the upper broken lines in Figs. 6 to 17) when the free-stream Mach number is raised, and the shock moves rearwards. When the Mach number has been raised to a value close to unity, so that the shock is at the trailing edge, the value of p_1 lies on the sonic-range pressure distribution. The p_1 locus and the sonic-range distribution thus coincide at the trailing edge, but it is necessary to consider the relation between the two curves over the remainder of the surface. The practical importance of this relation arises because a knowledge of the p_1 locus is of value in predicting the pressure distribution at high subsonic speeds, and there appear (*see* Ref. 13) to be good prospects of predicting the sonic-range distribution.

It is convenient to consider the pressure at a point P (Fig. 29) on the surface of an aerofoil beneath a local region of supersonic flow as being determined by two families of waves, one a family of expansion waves springing from the surface, and the other the compression waves resulting from the reflection of the first family at the sonic line. The contribution of the first family of waves to the pressure at P is determined by the surface slope at this point relative to the slope at the sonic point. The contribution of the second family depends in addition on the position of the sonic line, and on the velocity distribution in the local supersonic region. If the extent of, and the distribution within, the supersonic region ahead of the reflected compression wave striking P (Fig. 29) was independent of free-stream Mach number, the pressure at P would become equal to the value for the sonic-range pressure distribution as soon as the Mach number had been raised to a value for which the shock lies just downstream of P. Thus if this condition applied to all points on the surface, the p_1 loci shown in Figs. 6 to 17 would correspond with the sonic-range pressure distributions. The position of the sonic line must, however, change as the supersonic region extends laterally with increase of free-stream Mach number, and the position of the sonic point also moves when the Mach number is changed, thus altering the system of expansion waves originating from the surface. In general, therefore, the p_1 loci would not be expected to coincide with the sonic-range pressure distributions.

The observed position of the sonic point on the upper surface of the aerofoil is plotted in Fig. 30 against free-stream Mach number for several angles of incidence. At zero incidence, it is seen that the sonic point moves towards the leading edge as the Mach number is raised. Thus, as far as the contribution of the family of expansion waves is concerned, the sonic-range pressure at a point on the surface would be expected to be lower than the pressure p_1 at this point when

the shock wave has moved just behind it. The contribution of the reflected compression waves might be expected* to be greater at the lower free-stream Mach numbers, because the sonic line is closer to the surface, and this effect also gives values of p_1 which are high compared with the sonic range distribution, especially over the front part of the aerofoil. The result (*see* Fig. 6) is that the p_1 locus has pressures which are higher than those for the sonic-range distribution, the discrepancy, of course, decreasing as the trailing edge is approached.

When the aerofoil is at a positive incidence, the sonic point is, in general, seen from Fig. 30 to move aft when the Mach number is raised. As far as the contribution of the expansion waves originating from the surface is concerned, the values of p_1 at low values of the Mach number would, therefore, be expected to be lower than those at the same chordwise positions for the sonic-range pressure distribution. In other words, the p_1 locus would be expected to have, near the leading edge, pressures below the sonic-range pressures. This effect of the movement of the sonic point is opposed to some extent by the effect of the system of reflected compression waves which should, as discussed above, be strongest at the lower Mach numbers. Nevertheless, at large angles of incidence the p_1 locus is seen (in, for example, Fig. 13) to give pressures over the forward part of the aerofoil below the sonic-range pressures. At other angles of incidence (*see*, for example, Fig. 11) these opposing effects evidently cancel approximately, so that the p_1 locus and the sonic-range distribution are in reasonable agreement.

The movements of the sonic point discussed above result from movements of the stagnation point, and an analysis of the stagnation-point positions showed that the stagnation-point movements with Mach number and incidence were similar, but much smaller, than those of the sonic point.

Because of the effect of the family of compression waves running towards the surface, the local Mach number in the sonic-range pressure distributions is not constant over the flat portion of the surface at a level greater than that further forward, as it would be if the flow was of a simple-wave nature. Instead, the local Mach number rises to a maximum value well forward on the aerofoil, and then falls gradually as the trailing edge is approached. This effect is more pronounced on the present aerofoil than on the majority of those previously tested, because the surface is nearly flat over most of the chord, so that in this region there are no expansion waves springing from the surface to offset the effect of the incoming compressions. Also, the far-forward position of maximum thickness leads to relatively high surface curvature and strong expansions near the beginning of the supersonic region, which in turn are reflected at the sonic line as compression waves†.

Because of the shape of the sonic-range pressure distribution, and the differences between this distribution and the p_1 locus, the assumption of Section 2 that the local Mach number ahead of the shock is always lower than the sonic-range Mach number at the trailing edge is not strictly fulfilled on the present section. However, an examination of Figs. 6 to 9 shows that the assumption is not greatly in error for angles of incidence ($\alpha < 1\frac{1}{2}$ deg) for which separation would be expected to be absent.

7. *The Ratio p_2/p_1 of the Surface Static Pressures Downstream and Upstream of the Shock on the Upper Surface.*—If the equations for a normal shock wave applied, the static pressure p_2 just downstream of the shock could be calculated from the p_1 locus (*see* Section 6) for any specified chordwise position of the shock. It is, however, known that these equations cannot be used for this purpose for the shock wave formed on an aerofoil at high subsonic speeds, even when the shock is too weak to cause boundary-layer separation. This feature is illustrated in Fig. 31

* Neglecting any change in the reflected waves resulting from the change in the expansion waves incident on the sonic line due to the movement of the sonic point at the surface.

† Ref. 13 may be consulted for a more detailed discussion of these points.

where the ratio p_2/p_1 of the observed surface pressures just downstream and upstream of the shock (*see* sketch) is plotted against the upstream pressure p_1. It is seen that the points for different angles of incidence lie on separate curves, but that the curves for angles of incidence small enough for separation to be absent ($\alpha < 1\frac{1}{2}$ deg) are close together, and fall considerably below* the curve calculated from p_1 using the normal-shock equations.

Two explanations have been advanced to explain this discrepancy. The first[14] applies to curved surfaces, and argues that if the curvature is convex with respect to the flow, the static pressure must fall as the surface is approached in order to balance the centrifugal forces. This condition is satisfied ahead of the shock formed at the rear of the local region of supersonic flow, and the local Mach number ahead of the shock is accordingly greatest at the surface. If, however, the static pressure downstream of the shock was determined by the normal-shock equations, it would be greatest at the wall, and would fall as the distance from the wall increased. This condition is incompatible with convex curvature of the streamlines, so that the shock must be followed immediately by an expansion which is most intense at the surface, and reduces the pressure there below that for a normal shock. The second explanation[1, 15] for the relatively small pressure rise across the shock is that thickening of the boundary layer ahead of, and downstream of, the shock changes the Mach number ahead of the shock, and the stream-tube area downstream with respect to that upstream. Although, therefore, the shock-wave equations† apply across the shock, they do not relate the conditions at small distances upstream and downstream. Since the shock is on the flat part of the aerofoil surface for most of the points shown in Fig. 31 at low angles of incidence, it seems that the second explanation is more relevant in the present investigation.

A further possible explanation for the comparatively small observed pressure rise across the shock arises from the effects of the boundary layers on the side walls of the wind tunnel, and thus represents a possible defect in the arrangements used in this and other experiments on two-dimensional aerofoils at high subsonic speeds. Thickening of the side-wall boundary layers at the shock waves formed by the aerofoil will influence, to some extent, the pressures measured downstream of the shock on the aerofoil surface at mid-span. The magnitude of this effect is thought to depend on the shock strength, on the thickness of the side-wall boundary layer, and on the span of the aerofoil (about 1 in. and 14 in. respectively in the present experiment), but cannot be estimated reliably at present. Research is in hand to investigate this effect, but it is not anticipated that it will prove so large that the general conclusions of the present investigation are invalidated.

At larger angles of incidence separation occurs, and the shock becomes bifurcated. Except for cases where the shock lies close to the leading or trailing edge of the aerofoil, the majority of the points shown in Fig. 31 then lie close to the curve obtained for the separation of a flat-plate boundary layer at a normal shock. When, however, the shock is close to the leading edge, it is seen that the value of p_2/p_1 is abnormally high.‡ The reason for this anomaly is not fully understood, but it is thought that it is associated with the intense pressure gradient and, particularly, the associated flow deflection to which the boundary layer is subjected close to the nose of the aerofoil by the expansion waves springing from the surface and the reflected compression waves. Also, the chordwise length occupied by the pressure rise associated with the shock is quite large (about 0·02 to 0·05 chord) so that, if the reflected compression waves are intense, they may contribute an appreciable pressure rise over this distance which is included in the values plotted in Fig. 31, and also cause a significant deflection of the separated flow towards the surface.

---

* A linear relationship for the points for $1{\cdot}23 > M_1 > 1$ corresponds approximately to the equation $p_2/p_1 = 1 + 1{\cdot}67(M_1 - 1)$ whereas, for a weak normal shock, the shock-wave equations give (with $\gamma = 1{\cdot}40$) $p_2/p_1 \doteq 1 + 2{\cdot}33(M_1 - 1)$. Thus, the observed value of the pressure rise $(p_2 - p_1)$ across the shock is approximately 0·72 times the calculated value.

† Not necessarily the equations for a normal shock, since the thickening boundary layer ahead of the shock may result in the flow ahead of the shock being inclined to it at an angle differing from 90 deg.

‡ This feature has been observed on several aerofoils when the shock is near the leading edge.

No explanation can at present be advanced for the low values of the pressure ratio across the shock when it has moved back close to the trailing edge. However, it should be noted that, under these conditions, the pressure distribution downstream of the shock is poorly defined by the few available measurements, so that the value of p_2 cannot be estimated reliably. Moreover, the scatter of the observations in Fig. 31 about the curve for the flat plate is exaggerated by the open scale used, and is little larger than the scatter of the data obtained in the flat-plate experiments.

8. *The Pressure Recovery Between the Shock and the Static Hole at 0·965 Chord on the Upper Surface.*—Because of the effects of the slightly blunt trailing edge, it is convenient to consider separately the flow upstream of the last pressure hole (at 0·965 chord) on the upper surface, and between this hole and the trailing edge. Reference will be made to the pressure distributions plotted in Figs. 6 to 17, and to Fig. 32. Here the p_2 locus is plotted for a range of angles of incidence, and the pressure recovery downstream of the shock is represented by a straight line drawn at an angle equal to the mean observed pressure gradient, for a series of uniformly separated values of $p_{0\cdot965}$. The intercept between the p_2 locus and the mean curve of downstream pressure recovery indicates the shock position for the value of $p_{0\cdot965}$ under consideration, the shock positions being indicated by the short lines crossing the p_2 loci.

Since the slope of the surface of the section behind about 0·3 chord is small, the pressure gradient at small angles of incidence and low Mach number is relatively weak over this part of the section. Thus, as the shock moves back towards the nearly flat part of the section, there is a tendency, at small angles of incidence, for the mean pressure gradient between the shock and 0·965 chord to fall at first (*see*, for example, Fig. 8 and Fig. 32a for $\alpha = 1$ deg). However, when the shock is on the flat part of the section, the effects of the shock on the boundary layer result in a higher pressure gradient immediately behind the shock than further downstream, the flow pattern being envisaged as sketched in Fig. 33. Thus, with further rearwards movement of the shock, the average pressure gradient between the shock and 0·965 chord increases, since the relatively rapid pressure gradient behind the shock occupies a relatively larger proportion of the distance between the shock and 0·965 chord. This tendency for the pressure gradient behind the shock to be relatively large becomes particularly pronounced when separation occurs at the shock (*see*, for example, Fig. 11 and Fig. 32f for $\alpha = 3$ deg), where the pressure gradient between separation and reattachment is large compared with that along the surface when separation is absent. However, when the reattachment point moves downstream of 0·965 chord, the pressure at this point begins to fall rapidly so that the average pressure gradient downstream of the shock ceases to rise as the shock moves rearwards.

At larger angles of incidence (*e.g.*, Fig. 32h for $\alpha = 5$ deg), the flow is supersonic immediately behind the separation point, and the pressure distribution is then of the form sketched in Fig. 34, the pressure gradient at first being relatively weak, but increasing after the flow becomes subsonic because of the more rapid curvature of the streamlines towards the surface when this has occurred (*see* Refs. 2 and 3). As the separation bubble extends beyond 0·965 chord with increase of free-stream Mach number, the tendency is for the most rapid part of the pressure recovery to be lost first, so that the mean pressure gradient between the shock and 0·965 chord falls with rearwards movement of the shock (*see*, for example, Figs. 32h and 32i). When at $\alpha = 5$ deg or $\alpha = 6$ deg the shock has moved back close to the trailing edge, the mean pressure gradient downstream ceases to fall or increases slightly. This is attributed to the reduction of the size of the separated region as the separation point moves nearer to the trailing edge (*see* Ref. 2, p. 28), and to the fact that the values of p_2 increase towards the trailing edge so that the Mach number in the supersonic flow immediately behind the shock is lower, so that there is a tendency for the separation bubble to close more rapidly thus giving an increased pressure gradient.

9. *The Effects of the Shape of the p_2 Locus, and of the Downstream Pressure Recovery, on the Shock Position for a Given Pressure at 0·965 Chord on the Upper Surface.*— The effects of the shape of the p_2 locus, and of the mean pressure gradient downstream of the shock, on the shock position for a given value of the static pressure $p_{0\cdot965}$ near the trailing edge are illustrated in Fig. 32. Here the

shock positions are indicated by short lines crossing the p_2 loci, and are considered as being determined by the point of intersection of the p_2 locus, and the line of mean downstream pressure recovery, for the values of angle of incidence and $p_{0\cdot965}$ under consideration. The shock positions are plotted against $p_{0\cdot965}$ in Fig. 35.

Referring to Fig. 32, it is clear that the rate of shock movement with fall of $p_{0\cdot965}$ is inversely proportional to the difference between the slopes of the p_2 locus and the mean downstream pressure-recovery line. Thus, for example, the fact that the slope of the p_2 locus becomes increasingly negative towards the rear of the aerofoil at low angles of incidence, partially compensates the effect of the increasingly positive slope of the mean downstream pressure curve. Conversely, at large angles of incidence (*e.g.*, $\alpha = 5$ deg, 6 deg), the increasingly positive slope of the p_2 locus towards the trailing edge augments the effect of the increasing slope of the downstream pressure recovery line, and leads to rapid rearwards shock-wave movements with fall of $p_{0\cdot965}$.

The variation of shock position with the pressure near the trailing edge shown in Fig. 35 may thus be explained in terms of the changes of flow pattern that affect the p_2 loci and the pressure recoveries over the rear of the aerofoil. The relationship between this pressure and the free-stream pressure is discussed below.

10. *The Flow on the Upper Surface near the Trailing Edge and along the Wake.*—Since no pressure measurements were made in the wake, the flow near and downstream of the trailing edge is to some extent a matter for conjecture. The pressure distributions and flow patterns that are envisaged as taking place for a small angle of incidence ($\alpha = 1$ deg) are, however, sketched in Figs. 36 and 37. At low speeds, the flow pattern is of the type sketched in Fig. 37i, and the pressure falls as the trailing edge is approached as shown in the sketches of Fig. 36, and the measured distributions of Fig. 8. Downstream of the trailing edge, the pressure is thought to rise (by an amount greater than the pressure drop ahead of the trailing edge), as the stream tubes expand into the region behind the blunt trailing edge, until the boundary layers shed from the two surfaces unite. Thereafter, the pressure along the wake varies as sketched in Fig. 36. Because of the increase of pressure immediately downstream of the trailing edge, the values of the trailing-edge pressure are lower than they would be if the trailing edge were sharp (*see*, for example, the broken curve in Fig. 36), and, as seen in Fig. 40, the trailing-edge pressure is in fact less than the free-stream pressure. Because of the fall of pressure as the trailing edge is approached, the pressure $p_{0\cdot965}$ is higher (Fig. 40) than $p_{\text{T.E.}}$; it is also higher than p_0, but not by so great an amount as it would have been had the trailing edge been sharp. For a given value of p_0, one effect of the blunt trailing edge at low Mach number is, therefore, to reduce the pressures over the rear* of the upper surface as illustrated by the comparison between the full and broken lines in Fig. 36. Because of the small trailing-edge thickness, this effect is not large for the present aerofoil.

When the value of p_0 is reduced, there is at first no substantial change in the flow pattern over the rear of the aerofoil, and both $p_{\text{T.E.}}$ and $p_{0\cdot965}$ vary almost linearly with p_0 (Fig. 40). When, however, p_0/H_0 falls below about $0\cdot58$, both $p_{\text{T.E.}}$ and $p_{0\cdot965}$ begin to fall less rapidly as p_0 is reduced. It is thought that this occurs when the boundary-layer thickness near the trailing edge first begins to increase markedly as a result of the effect of the shock wave on the upper surface. The effect of the blunt base would be expected to decrease as the rate of boundary-layer growth (*i.e.*, the angle between the edge of the boundary layer and the surface), and the ratio of the boundary-layer thickness at the trailing edge to the trailing-edge thickness increase. Thus when p_0/H_0 is reduced to about $0\cdot58$, the pressure drop immediately upstream of the base falls, and, presumably, the pressure rise behind the trailing edge also falls as illustrated in Figs. 36(ii) and 37(ii). As a result

* The comparison in Fig. 5 between the measured pressures and those calculated for a sharp trailing edge suggests that the effects of the blunt trailing edge do not extend far forward.

$p_{T.E.}$ ceases to be less than p_0 and rises above it, and the rate of fall of $p_{0.965}$ is correspondingly reduced; eventually (Fig. 36(ii), 37(ii) and Fig. 40) $p_{T.E.}$ and $p_{0.965}$ become approximately equal at a value greater than p_0.

With further decrease of p_0, the shock moves back close to the trailing edge (*see* Fig. 36(iii)), and the region of relatively strong positive pressure gradient extends into the wake. The pressure immediately downstream of the trailing edge then once more increases along the wake, and the value of $p_{T.E.}$ begins to fall rapidly when p_0 is reduced (Fig. 40). Because of the relatively strong pressure gradient between 0·965 chord and the trailing edge, $p_{0.965}$ falls even more rapidly, as shown in Fig. 40. The rate of fall of $p_{T.E.}$ becomes particularly rapid when the flow at the trailing edge becomes supersonic, since the pressure along the wake then rises instead of falling (Fig. 36(iv) and Fig 40). As the shock moves downstream of 0·965 chord, the pressure there becomes roughly constant at a value corresponding to the ' sonic-range ' value as shown in Fig. 40. When the value of p_0 is low enough* for an inclined shock to exist near the trailing edge (Figs. 36(v) and 37(v)), the base-pressure effect reappears, and $p_{T.E.}$ falls to a value considerably below $p_{0.965}$ as shown in Fig. 40.

The example considered above was for an angle of incidence for which separation was absent, and a larger angle of incidence ($\alpha = 5$ deg) is now considered to illustrate the behaviour when separation is present. Because of the increased boundary-layer thickness near the upper-surface trailing edge, the effects of the blunt trailing edge are not so pronounced at low speeds as they were at $\alpha = 1$ deg, and (*see* Fig. 38 and Fig. 42) $p_{0.965}$ and $p_{T.E.}$ are more nearly equal. When p_0 decreases, the value of $p_{T.E.}$ approaches p_0 gradually, because the boundary-layer thickness at the trailing edge increases due to the effect of the shock; this effect is, however, seen in Fig. 42 to be small. As discussed in Section 8, the pressure gradient along the bubble of separated flow increases when the flow outside the bubble becomes subsonic, so that the pressure gradient behind the shock is at first relatively gradual whilst the main-stream flow is supersonic, but becomes stronger further downstream where the flow is subsonic; finally, after reattachment, the pressure gradient is again reduced. When the separation bubble first extends into the wake, the pressures downstream of the trailing edge thus increase quite rapidly as sketched in Fig. 38(ii) until the bubble closes (Fig. 39 (ii)), so that the net pressure drop along the wake between the trailing edge and a point far downstream is reduced or reversed in sign. The value of $p_{T.E.}$ thus begins to fall rapidly with decrease in p_0 as shown in Fig. 42. As for $\alpha = 1$ deg, the value of $p_{0.965}$ drops even more rapidly because of the strong pressure gradient between 0·965 chord and the trailing edge. However, as the bubble extends further into the wake with decrease of p_0, the region of reduced pressure gradient associated with the supersonic external flow moves downstream of the trailing edge (Fig. 38 iii)). The rate of fall of $p_{T.E.}$ with respect to p_0 is then reduced as shown in Fig. 42. Eventually, when the shock is just ahead of the trailing edge and becomes inclined to the stream, the pressure rise across the shock decreases, and $p_{T.E.}$ falls rapidly. Subsonic flow is then restored through a normal shock downstream of the trailing edge (Fig. 38 iv)). This shock moves downstream and weakens as the free-stream Mach number approaches unity, as discussed in detail in Ref. 4. Eventually, when the shock on the aerofoil reaches the trailing edge, the pressure there would become approximately constant as it did at $\alpha = 1$ deg, but for $\alpha = 5$ deg the free-stream Mach number could not be raised to a sufficiently high value to achieve this condition. When the shock moved past 0·965 chord, the pressure there would also become nearly constant at the sonic-range value, but the free-stream Mach number again did not reach a value sufficiently high to achieve this condition. At $\alpha = 3$ deg (Fig. 41) the variations of $p_{T.E.}$ and $p_{0.965}$ with p_0 show similar features to those at $\alpha = 5$ deg, but in this case the Mach number could be raised sufficiently for the pressures to reach nearly constant values.

11. *The Variation of the Upper-Surface Shock Position with the Free-Stream Static Pressure p_0.*— It has been seen in Fig. 35 that, especially at large angles of incidence, the shock position on the

* When the free-stream Mach number is slightly less than unity (*i.e.*, lies between the values corresponding to curves (iii) and (iv) in Fig. 36), a nearly normal shock wave is present downstream of the trailing edge as shown in Fig. 38, curve (iv).

upper surface varies in an erratic manner with the pressure $p_{0\cdot965}$ just ahead of the trailing edge, and it has been noted in Section 9 that the irregularities may be explained in terms of the variations in the pressure p_2 downstream of the shock, and in the mean pressure gradient between the shock and 0·965 chord. The relationship between shock position and free-stream Mach number involves, however, not only the factors considered above, but also the variation of $p_{0\cdot965}$ with the free-stream pressure p_0 (*i.e.*, the flow near the trailing edge and along the wake). When allowance is made for these factors, the shock-wave movement occurs more smoothly as illustrated in Fig. 43, where the shock position is plotted against free-stream Mach number. The reasons for this reduction of the irregularities in the curves of shock-wave position follow from the discussion of Section 10, and are illustrated in Fig. 44 where it is seen that the irregularities in the variation of $p_{0\cdot965}$ with p_0 ,and in shock position with $p_{0\cdot965}$ occur at the same values of $p_{0\cdot965}$.

The shock position for a given value of p_0 may be considered (on the lines of Section 5.1) as being determined by the intersection between the p_2 locus, and the curve representing the pressure change between the p_2 locus and the pressure p_0 far downstream of the aerofoil. Thus, the shock position might be expected to move smoothly with p_0 if the p_2 locus is smooth, and the average pressure gradient between the shock and a point far downstream of the aerofoil (*i.e.*, between p_2 and p_0) varies smoothly with p_0. Because of the large extent of flat surface, the p_2 loci for the present aerofoil are seen in Fig. 32 to be relatively smooth, even at large angles of incidence. Also, it has been suggested in Section 10 that the pressure distribution over the bubble of separated flow is broadly similar (*see* Fig. 38) when the bubble extends into and closes in the wake, as when it closes on the surface. In other words, the pressure distribution behind the shock moves, without abrupt changes, downstream with the shock, although the values of the pressures at fixed points (*e.g.*, at 0·965 chord) under the pressure distribution vary. The result is that, for a given value of the angle of incidence, the shock movement with fall of free-stream pressure p_0 occurs relatively smoothly, although the value of $p_{0\cdot965}$ shows abrupt changes.

This relatively smooth movement of the upper-surface shock with p_0 is in contrast to the results obtained on many previously tested aerofoils. This is largely because the values of the surface slopes of these aerofoils have given values of p_1 which decrease continuously as the shock moves along the surface. Frequently, therefore, the shock is too weak to provoke separation when it is near the leading edge, but becomes strong enough to do so when p_0 is reduced, and the shock has moved further aft. The result is that the p_2 locus frequently changes abruptly in the region where the shock becomes strong enough to cause separation, and that when separation occurs the pressure distribution behind the shock also changes. The fact that p_1 continues to fall with increase of free-stream Mach number after the onset of separation also has important effects on the development of the separated flow on these aerofoils (*see* Ref. 2), which are absent for the present section.

It should be noted that the smooth rearwards movement of the upper-surface shock on the present aerofoil occurs only when the Mach number is raised at a fixed angle of incidence, and not when the incidence is increased at constant Mach number. In the latter case the shock wave becomes strong enough to provoke separation at some stage in its rearwards movement, and the effects on the p_2 locus and downstream pressure recovery then ultimately lead to the reversal, observed on many previous aerofoils, in the direction of shock-wave movement with increasing incidence as illustrated in Fig. 45. The variation of the value of p_2 at the shock is shown in Fig. 46. If the mean pressure gradient between the shock and a point far downstream did not change with angle of incidence, the shock wave would be expected to move aft if p_2 increases with incidence, and to move forwards if p_2 decreases (*see* Section 5.1 and Fig. 28). In practice, the mean downstream pressure gradient also changes with incidence, but it is seen in Fig. 46 that the value of p_2 falls rapidly over the range of incidence in which the direction of shock movement changes sign for Mach numbers between 0·8 and 0·9. For higher Mach numbers, the observed shock movements cannot be explained in terms of changes in the pressure p_2, and it is concluded that changes in the downstream pressure gradient play a dominant part.

12. *The Relationship between the Flows on the Upper and Lower Surfaces.*—In previous discussions of the effects of separation on the flow past aerofoils, it has been argued that, since the wake can support no appreciable transverse pressure gradient, the static pressure at the trailing edge must be substantially the same on the upper surface as on the lower surface. As discussed in Section 5.1, the requirement that this condition must be satisfied is considered to be of fundamental importance in governing the relation between the flows over the two surfaces and, in particular, in determining the flow changes on the lower surface that result from separation on the upper surface. These rapid flow changes on the lower surface have usually been found to begin when the trailing-edge pressure diverges (*i.e.*, begins to fall rapidly with respect to the free-stream pressure as shown in Figs. 40 to 42), as a result of the rearwards extension of the bubble of separated flow formed on the upper surface. The boundary for the divergence of the trailing-edge pressure on the present aerofoil is plotted, on a free-stream Mach-number, angle-of-incidence basis, in Fig. 23. It will be seen that over a certain range of incidence the trailing-edge pressure diverges even though separation is absent, because (*see* Section 10) of the effects of boundary-layer thickening behind the upper-surface shock. The effects of this divergence of the trailing-edge pressure, and other aspects of the relationship between the flows on the upper and lower surfaces, will be discussed by considering Figs. 40 to 42 which show the values of the pressure $p_{0\cdot9}$ measured at the most downstream pressure hole (at $0\cdot9$ chord) on the lower surface and of the pressure $p_{0\cdot5}$ at $0\cdot5$ chord on the lower surface, together with the pressure $p_{\text{T.E.}}$ at the trailing edge and the pressure $p_{0\cdot965}$ at the rear of the upper surface.

At a small angle of incidence (*see* Fig. 40 for $\alpha = 1$ deg), the flow just ahead of the trailing edge would, at low Mach number, be expected to be similar on the upper and lower surfaces. This is confirmed by the agreement between the pressures at $0\cdot965$ chord on the upper surface, and $0\cdot9$ chord on the lower surface. For the reasons discussed in Section 10, both pressures are higher than the trailing edge pressure. When the rate of fall of trailing-edge pressure with p_0 decreases, as a result of the effects of the shock wave on the upper-surface boundary layer, the rates of fall of $p_{0\cdot9}$ and $p_{0\cdot5}$ on the lower surface are also reduced, but less markedly, because the effects of the acceleration round the blunt trailing edge decay with increasing distance ahead of the trailing edge, and have become relatively small when this distance is $0\cdot1$ chord. When, however, the Mach number has been raised to about $0\cdot98$ ($p_0/H_0 \simeq 0\cdot54$), the effect of the lower-surface shock on the boundary-layer thickness at the trailing edge of the lower surface has evidently become sufficient to reduce considerably the expansion of the flow on the lower surface round the trailing edge. The pressure $p_{0\cdot9}$ on this surface is then approximately equal to $p_{\text{T.E.}}$, and falls rapidly with it. Since the lower-surface shock moves past $0\cdot5$ chord before the conditions described above are reached (the corresponding part of the curve for $p_{0\cdot5}$ is shown dotted in Fig. 40), it is not possible to see from Fig. 40 whether the rapid fall of trailing-edge pressure is accompanied by a general fall of the pressures over the lower surface. However, reference to Fig. 43 shows that there is apparently a small increase in the rate at which the lower-surface shock moves aft with reduction of p_0, when p_0 has fallen to about $0\cdot54$. The flow at the trailing edge is seen in Fig. 40 to become sonic soon after the trailing-edge pressure diverges, and before it has fallen to a value below that corresponding to the nearly linear variation with p_0 which occurs over most of the Mach-number range. Since, when the flow is sonic at the trailing edge, a local expansion can occur there on the lower surface, the pressures just ahead of the trailing edge need no longer be equal on the two surfaces. Thus, the effect of the falling trailing-edge pressure on the flow over the lower surface is present for only a small range of Mach number, and within this range is quite small because of the small change of trailing-edge pressure.

The fall of $p_{0\cdot9}$ which accompanies the fall of $p_{\text{T.E.}}$ (Fig. 40) soon becomes confused with that associated with the passage of the lower-surface shock past $0\cdot9$ chord and, with further reduction of p_0, the pressure $p_{0\cdot9}$ becomes nearly constant at its sonic-range value.

At a larger angle of incidence there is a marked acceleration of the flow on the lower surface between $0\cdot9$ chord and the trailing edge (*see*, for example, Fig. 13 for $\alpha = 5$ deg), and the value of $p_{0\cdot9}$ is seen in Fig. 42 to be higher than $p_{\text{T.E.}}$ or $p_{0\cdot965}$ at low Mach numbers. When the nearly linear variation of $p_{\text{T.E.}}$ with p_0 changes, the variation of $p_{0\cdot9}$ is modified only slightly, because the

effects on the lower surface are confined to the part of the chord just ahead of the trailing edge. There is thus an increase in the acceleration over this part of the chord which compensates for the falling trailing-edge pressure resulting from the rearwards extension of the separation bubble on the upper surface. The pressures well upstream of the trailing edge (*see* curve for $p_{0\cdot5}$ in Fig. 42) are thus hardly affected when the trailing-edge pressure diverges. This effect is also seen at other angles of incidence (*see*, for example, Figs. 11 and 41 for $\alpha = 3$ deg), and becomes less pronounced as the angle of incidence is reduced. It has also been observed[2] on other aerofoils when the angle of incidence is sufficiently large for the lower surface to be inclined downwards at the trailing edge relative to the free stream. The fact that, under these conditions, the flow on the lower surface is only affected locally by the fall of trailing-edge pressure, has an important bearing on the effects of upper-surface flow separation on the force and moment coefficients acting on the aerofoil (*see* Section 13).

Another consequence of the rapid acceleration of the flow on the lower surface just ahead of the trailing edge, is that sonic flow occurs at the trailing edge relatively early in the development of the flow over the lower surface with increasing free-stream Mach number. This effect is illustrated in Fig. 41 (and less clearly in Fig. 42), where it is seen that the tendency for $p_{0\cdot9}$ and $p_{0\cdot5}$ to follow the rapid fall of $p_{\text{T.E.}}$ disappears when $p_{\text{T.E.}}$ reaches the value corresponding to sonic flow. At angles of incidence greater than about 3 deg, sonic flow occurs in the rapidly accelerating flow near the trailing edge before a region of supersonic flow and a shock wave is formed further forward on the section. Under these circumstances, the flows on the two surfaces have become independent before a shock wave is formed on the lower surface, so that the subsequent rearwards movement of this shock is largely uninfluenced by the development of the separated flow on the upper surface.

As shown in Fig. 47 there is, at angles of incidence greater than 2 deg, a range of free-stream Mach number for which two sonic points are present on the lower surface, one near the leading edge and the other near the trailing edge. In these circumstances there may be two shocks on the lower surface, as illustrated in Fig. 48, one ahead of the trailing edge and other downstream of it. When the free-stream Mach number is raised, both sonic points are seen in Fig. 47 to move towards the leading edge, but the rearward sonic point moves much more rapidly and thus overtakes the forward one, so that at Mach numbers a little greater than unity there is only a single sonic point near the leading edge. The rapid forward movement of the rear sonic point is accompanied by a rapid extension of low pressure over the lower surface. For the angles of incidence ($\alpha = 2$ deg and $\alpha = 3$ deg) for which the Mach-number range of the tunnel permitted the sonic-point movement to be followed in detail, the resulting effect on the loading on the aerofoil (*see* Section 13) was, however, not large because (*see* Figs. 10 and 11) the lower-surface shocks are weak. At larger angles of incidence the effect may, however, be more significant.

The lower-surface-shock positions are plotted against free-stream pressure in Fig. 43, and for the reasons discussed above it is seen that the shock-wave movement occurs relatively smoothly, even when extensive separation is present on the upper surface. It is also seen that, for all values of the free-stream Mach number, the lower-surface shock lies upstream of the shock on the upper surface, so that when the Mach number is raised the upper-surface shock reaches the trailing edge first, as illustrated in the example reproduced in Fig. 49. This result is at variance with those for all previously tested sections known to the authors where, as a result of the effects of boundary-layer separation occurring at the upper-surface shock, the lower surface shock has reached the trailing edge first. The present result was anticipated[2] in the absence of separation on the basis of an argument which may be summarized by referring to Fig. 28. If the section is symmetrical, the values of p_1 will be lower on the upper surface than on the lower, so that if separation is absent the values of p_2 will be greater on the upper surface. Also, if separation is absent, the mean pressure gradient between the shock and the trailing edge would be expected to be greater on the upper surface. Thus if, for a given value of the pressure at the trailing edge (*i.e.*, a given

value of p_0), the shock position is considered as being determined by the intersection between the p_2 locus and the curve of mean downstream pressure recovery, the shock must lie further aft on the upper than on the lower surface. On most previously tested sections the value of p_1 decreases relatively rapidly as the upper-surface shock moves aft, so that at some stage the shock becomes strong enough to provoke separation, and the value of p_2 falls to a value which is frequently less than that at the same chordwise station on the lower surface. The p_2 loci thus cross, and this phenomenon, coupled with a change in the pressure recovery downstream of the upper-surface shock, results in a rearwards movement of the lower-surface shock which exceeds that for the upper surface.

13. *The Effects of the Changes of Pressure Distribution on the Loading on the Aerofoil.*—The changes in the pressure distribution over the aerofoil when the Mach number is raised affect the force and moment coefficients, and these effects are discussed briefly below. In order to demonstrate the individual contributions of the pressures acting on the upper and lower surfaces, it is convenient to separate the contributions of the two surfaces to the lift coefficient as shown in Figs. 50 to 53.

When, at a small angle of incidence (*see* Fig. 50 for $\alpha = 1$ deg), the Mach number is raised, there is at first a fairly rapid increase in the suction force* on both surfaces, but, since this increase occurs approximately equally on both surfaces, the value of C_L (Fig. 18) increases only slowly. The suction force on the upper surface increases more rapidly, however, when supersonic flow appears on the surface and extends rearwards with increasing free-stream Mach number. The value of C_L thus increases more rapidly, and the rate of increase is not greatly affected when supersonic flow appears on the lower surface, because the local Mach numbers there are relatively low. The suction force on the upper surface continues to increase until the trailing-edge pressure diverges. Thereafter, a reduction in the rate of rearwards shock movement, and hence of the rearwards extension of the lower pressures in the supersonic region, reduces the rate of increase of the upper-surface contribution to C_L. Simultaneously, there is an increase in the rate of rearwards movement of the lower-surface shock (*see* Section 12), so that the suction force on the lower surface increases. The value of C_L thus begins to fall fairly rapidly until both shocks have reached the trailing edge, and the sonic-range pressure distributions have extended over the whole of both surfaces. Thereafter, the pressures over the aerofoil are insensitive to Mach number, and C_L is approximately inversely proportional to the quantity $\frac{1}{2}\rho U^2$.

At a larger angle of incidence (Fig. 51 for $\alpha = 3$ deg), there is again a rapid increase in the suction force acting on the upper surface after sonic flow occurs, so that the value of C_L rises. The rate of increase is reduced after the trailing-edge pressure diverges, and simultaneously the pressures over the lower surface begin to fall more rapidly (*see* Fig. 41), so that C_L soon begins to decrease. Sonic flow occurs at the trailing edge, and the upper-surface shock moves nearly to the trailing edge before a shock appears on the lower surface, so that the lower-surface shock does not move back very rapidly in response to the falling trailing-edge pressure. The value of C_L thus falls steadily with increase of Mach number because of the rearwards shock movement on the lower surface and the increasing value of $\frac{1}{2}\rho U^2$.

At an even larger angle of incidence (*see* Fig. 52 for $\alpha = 5$ deg) the suction force on the lower surface varies smoothly with Mach number (*see* Section 12), and the changes in the suction force on the upper surface are in general similar to those discussed above. The value of C_L thus varies with Mach number in a similar manner to that at lower incidence.

For an angle of incidence (*see* Fig. 53 for $\alpha = 8$ deg) for which leading-edge separation is present at low Mach number, the suction force on the upper surface begins to increase rapidly when the Mach number is raised to a sufficiently high value to lead to flow attachment round the nose, because of the formation of a region of low-pressure supersonic flow over the forward part of the

* For brevity, and to avoid confusion concerning the signs of the contributions of the two surfaces to the lift coefficient, the values of the ordinate in Figs. 50 to 53 for each surface is referred to as the suction force acting on that surface.

upper surface*. For the reasons discussed in Section 7, the pressure p_2 behind the shock is highest near the leading edge, so that the p_2 locus (*see* Fig. 16) falls over the forward part of the aerofoil, and the rate of rearwards movement of the upper-surface shock (*see* Fig. 43) with increase of Mach number is at first quite gradual (*see* Section 5.1 and Fig. 28). The rate of increase of the suction force on the upper surface is thus reduced, and, because of the effect of increasing $\frac{1}{2}\rho U^2$, and of the steadily increasing suction force on the lower surface (Fig. 53), the value of C_L begins to fall with increasing Mach number until $M_0 \simeq 0{\cdot}85$. At higher Mach numbers the shock lies further away from the leading edge where the p_2 locus corresponds, not to a rapidly falling pressure, but to a pressure that rises gradually (Fig. 16). Thus, as shown in Fig. 43, the upper-surface shock begins to move back more rapidly with increase of Mach number when M_0 exceeds about $0{\cdot}85$, and the value of C_L begins to increase again. Because of the effects discussed in Section 12, the suction force on the lower surface is seen in Fig. 53 to increase smoothly with Mach number, and is not apparently affected by changes in the upper-surface flow.

Because (*see* Section 13) the lower-surface shock always moves back to the trailing edge less rapidly than the upper-surface shock when the Mach number is raised, the values of C_L for angles of incidence up to 3 deg are seen in Fig. 18 to fall monotonically after rising to their maximum values. This is in contrast to the behaviour of many aerofoil sections (*see* Refs. 1 and 2) where, because of the effects of upper-surface flow separation, the lower-surface shock moves back to the trailing edge first, and the resultant extension of low pressures over the lower surface leads to a trough in the lift curve at a Mach number somewhat above that for the maximum value of C_L.

The effects of the changes of pressure distribution on the pitching-moment coefficient and the centre-of-pressure position may be explained by arguments similar to those used above for the lift coefficient. A striking feature, for angles of incidence where separation is absent, is that when the Mach number is raised the pitching-moment coefficient decreases to a large nose-down value before rising again to a value typical of supersonic flow. There is a corresponding movement of the centre of pressure aft of the value in supersonic flow. These results were anticipated, because it was expected (*see* Section 12) that the upper-surface shock would move aft more rapidly than, and reach the trailing edge before, the shock on the lower surface. After the upper-surface shock reaches the trailing edge, the pitching-moment coefficient must rise (become more strongly nose-up) with further increase of Mach number, because the movement of the lower-surface shock towards the trailing edge results in an extension of low pressures over the lower surface aft of the quarter-chord point. Thus, when the Mach number is raised, the value of C_m for the condition when both shocks lie at the trailing edge must be approached from a more negative value, and, since the value of C_m at low Mach number exceeds that in supersonic flow, the curve of C_m against M_0 must pass through a minimum.

The form-drag coefficients obtained by integrating the pressures acting perpendicular to the surface are plotted against free-stream Mach number in Fig. 21, which also includes a curve showing the conditions for which sonic flow first occurs at the crest† of the upper surface. At low angles of incidence it is seen that the occurrence of sonic flow at the crest agrees well with the beginning of the drag rise, because this is due mainly to the extension behind the crest of the low pressures in the local region of supersonic flow. At larger angles of incidence, the drag rise is due initially to a reduction of the suction acting over the leading edge, and occurs before sonic flow appears at the crest. These matters are discussed in greater detail with reference to the present results and those obtained on other aerofoils in Ref. 16.

14. *Concluding Remarks.*—The results of the investigation support the suggestion that the value of the flow-deflection angle at the trailing edge is an important design parameter that determines whether shock-induced separation occurs at transonic speeds, and show that this angle must be very small (< 3 deg) if separation is to be avoided. It follows that separation will

* This effect also leads to a nose-up change in the trend of the pitching-moment curve, as shown in Fig. 19.

† The point on the upper surface where the tangent to the surface is parallel to the direction of the undisturbed stream.

frequently occur at transonic speeds even on thin sections, although the effects may be considerably less severe than those encountered previously for thicker sections.

When separation is absent, the thickening of the boundary layer at the upper-surface shock, and its subsequent development have been shown to have effects that are in many ways similar to those of shock-induced separation. The magnitudes of these effects are, however, relatively small, and features such as a movement of the shock towards the trailing edge that occurs more rapidly on the lower than on the upper surface do not result. The prediction of the pressure distribution in the presence of viscous effects is considered to require methods for estimating the static pressure immediately upstream of the shock, the static-pressure distribution through and downstream of the shock in the presence of the boundary layer, and the static-pressure distribution downstream of the aerofoil including viscous effects arising from the presence of the wake. Some progress has been made in the investigation of these factors, but much further work is clearly necessary before a satisfactory method of prediction can be devised.

At large angles of incidence, it has been seen that when the free-stream Mach number is raised, the flow pattern changes more smoothly than for most previous sections. This is attributed to the fact that the local Mach number immediately ahead of the shock does not increase markedly as the shock moves aft, so that shock-induced separation is present for almost the whole range of shock positions, and does not occur when the shock has moved aft by a certain amount. Moreover, even when separation occurs, the fact that the local Mach number ahead of the shock does not increase as the shock moves aft, avoids any substantial increase of the severity of separation with increasing free-stream Mach number. Also, as a result of the small trailing-edge angle, a rapid acceleration occurs along the rear of the lower surface, and it has been shown that this makes the flow over the major part of the lower surface relatively insensitive to changes of the upper-surface flow.

As regards the practical significance of the results, the confirmation of the simple method for predicting whether separation will occur on a given aerofoil, and the demonstration that separation-free flow may be achieved at all Mach numbers for lift coefficients up to at least $0{\cdot}25$, is considered to be valuable. The relatively smooth changes of flow pattern with free-stream Mach number for the larger angles of incidence is considered to be of less practical significance, partly because the changes occur less smoothly when the angle of incidence is changed, and partly because phenomena such as buffeting may preclude the use of large incidences.

15. *Acknowledgements.*—Mr. P. J. Peggs assisted with the experimental work, and Mrs. N. A. North with the analysis of the results. The form-drag coefficients were evaluated by Mr. Wilkinson of the de Havilland Aeroplane Co. The model was constructed at the N.P.L. by Mr. W. Haywood. The authors wish to thank their colleagues Dr. G. E. Gadd and Mr. H. H. Pearcey for helpful discussions, and suggestions made during the course of the work.

LIST OF SYMBOLS THAT OCCUR FREQUENTLY

p	Static pressure
p_0	Static pressure in the undisturbed stream
p_1	Static pressure just ahead of the shock
p_2	Static pressure just behind the shock
$p_{\text{T.E.}}$	Static pressure at the trailing edge
$p_{0\cdot965}$	Static pressure at $0{\cdot}965$ chord on the upper surface
$p_{0\cdot9}$	Static pressure at $0{\cdot}9$ chord on the lower surface
$p_{0\cdot5}$	Static pressure at $0{\cdot}5$ chord on the lower surface
H_0	Total head of the undisturbed stream
M	Local Mach number
M_0	Free-stream Mach number

REFERENCES

No.	*Author*	*Title, etc.*
1	D. W. Holder, H. H. Pearcey and G. E. Gadd (N.P.L.), and J. Seddon (R.A.E.)	The interaction between shock waves and boundary layers (with a note on 'The effects of the interaction on the performance of supersonic intakes'). C.P. 180. February, 1954.
2	H. H. Pearcey	Some effects of shock-induced separation of turbulent boundary layers in transonic flow past aerofoils. Proceedings of the N.P.L. Symposium on Boundary Layers. H.M.S.O. 1955.
3	D. W. Holder	The interaction between shock waves and boundary layers. Proceedings of the 5th International Aeronautical Conference. Institute of Aeronautical Sciences. 1955.
4	D. W. Holder	Note on the flow near the tail of a two-dimensional aerofoil moving at a free-stream Mach number close to unity. C.P. 188. June, 1954.
5	R. C. Pankhurst	N.P.L. Aerofoil Catalogue and Bibliography. C.P. 81. July, 1951.
6	L. H. Tanner	Curves suitable for families of aerofoils with variable maximum thickness position, nose radius, camber and nose droop. C.P. 358. February, 1957.
7	C. S. Sinnott	On the prediction of mixed subsonic/supersonic pressure distributions over aerofoils. Part III Analysis of theoretical solutions.
8	L. C. Woods	The application of the polygon method to the calculation of the compressible subsonic flow round two-dimensional profiles. C.P. 115. June, 1952.
9	J. R. Spreiter and A. Alksne ..	Theoretical prediction of pressure distributions on nonlifting airfoils at high subsonic speeds. N.A.C.A. Report 1217. 1954. Supersedes N.A.C.A. Tech. Note 3096. 1954.
10	A. B. Haines (R.A.E.), D. W. Holder and H. H. Pearcey (N.P.L.)	Scale effects at high subsonic and transonic speeds and methods for fixing boundary-layer transition in model experiments. R. & M. 3012. September, 1954.
11	D. W. Holder and G. E. Gadd ..	The interaction between shock waves and boundary layers. Proceedings of the N.P.L. Symposium on Boundary Layers. H.M.S.O. 1955.
12	B. D. Henshall and R. F. Cash ..	The interaction between shock waves and boundary layers at the trailing edge of a double-wedge aerofoil at supersonic speed. R. & M. 3004. March, 1955.
13	C. S. Sinnott	On the flow of a sonic stream past an aerofoil surface leading to a semi-empirical method for the prediction of sonic-range pressure distributions. A.R.C. 19,169. F.M. 2526. April, 1957.
14	J. Ackeret, F. Feldmann and N. Rott	Investigations of compression shocks and boundary layers in fast moving gases. Institut für Aerodynamik E.T.H. Zurich. Report No. 10. 1946. (Translated as A.R.C. 10,014.)
	See also H. W. Emmons	The theoretical flow of a frictionless, adiabatic perfect gas inside of a two-dimensional hyperbolic nozzle. N.A.C.A. Tech. Note 1003. 1946.
15	G. E. Gadd..	The interaction between a weak normal shock wave and a turbulent boundary layer.
16	H. H. Pearcey	The influence of section shape on the compressibility drag rise of two-dimensional aerofoils. (In preparation.)

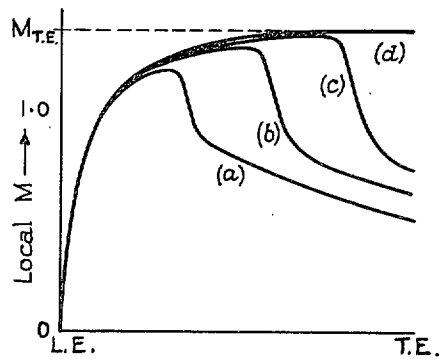

FIG. 1. The distributions of local Mach number along the chord of an aerofoil for increasing free-stream Mach number ((*a*) to (*d*)).

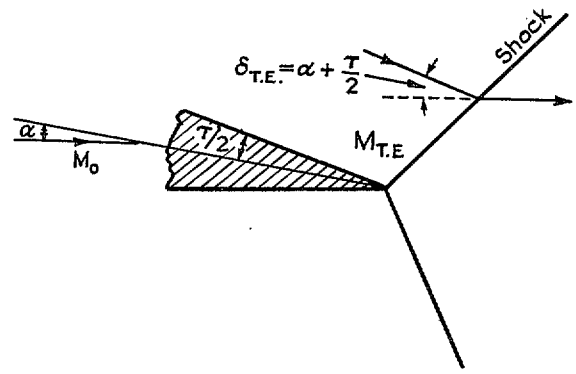

FIG. 2. The flow near the trailing edge for a free-stream Mach number close to unity (Curve (*d*) in Fig. 1), illustrating the notation used in Fig. 3.

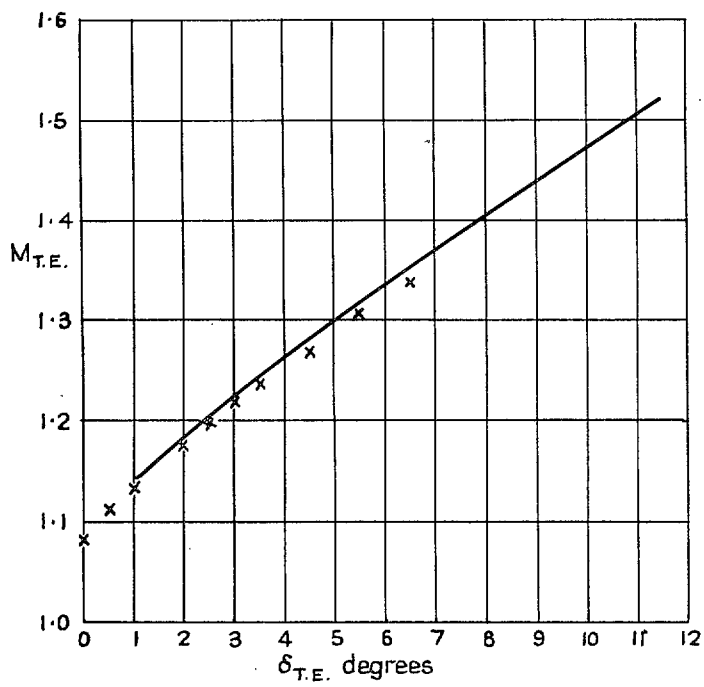

FIG. 3. The experimental relationship between the trailing-edge Mach number and deflection angle.

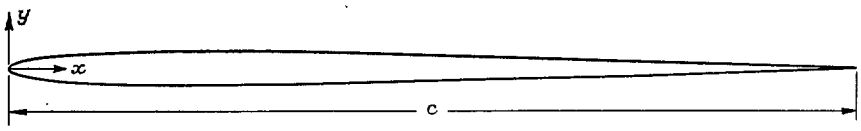

Table 1
Coordinates of the section.

x/c	y/c	x/c	y/c
0	0	0·1278	0·0188
0·0011	0·0026	0·1583	0·0196
0·0022	0·0036	0·1917	0·0199
0·0029	0·0047	0·2334	0·0198
0·0065	0·0060	0·2889	0·0192
0·0111	0·0076	0·3611	0·0178
0·0178	0·0093	0·5000	0·0144
0·0267	0·0110	0·7440	0·0079
0·0389	0·0127	Straight	
0·0556	0·0145	1·000	0·0011
0·1000	0·0176		

Table 2
Values of x/c at the pressure holes

Upper surface		Lower surface	
0·0015	0·3900	0	0·8000
0·0030	0·4700	0·0100	0·9000
0·0065	0·5500	0·0500	
0·0150	0·6300	0·1000	
0·0200	0·7100	0·1665	
0·0350	0·7900	0·2330	
0·0750	0·8700	0·3330	
0·1000	0·9300	0·4110	
0·1500	0·9650	0·5000	
0·2300	1·0000	0·6000	
0·3100		0·7000	

c = 9·00 inches. Trailing-edge angle = 3·024 degrees. Maximum thickness = 0·04c at x/c = 0·2.
Nose radius = 0·003c

FIG 4a. Details of the aerofoil section (NPL 491).

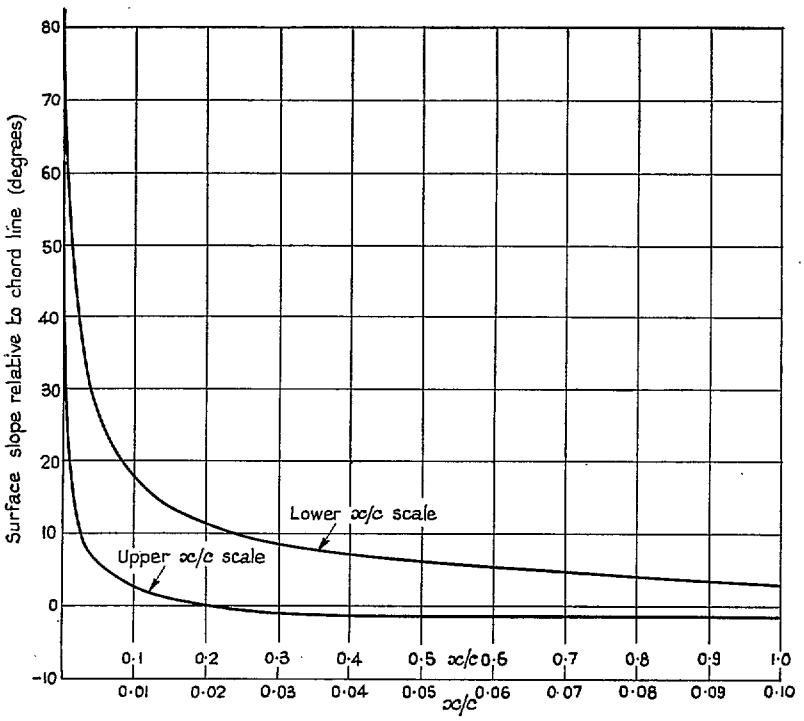

FIG. 4b. Surface slopes of the section (NPL 491).

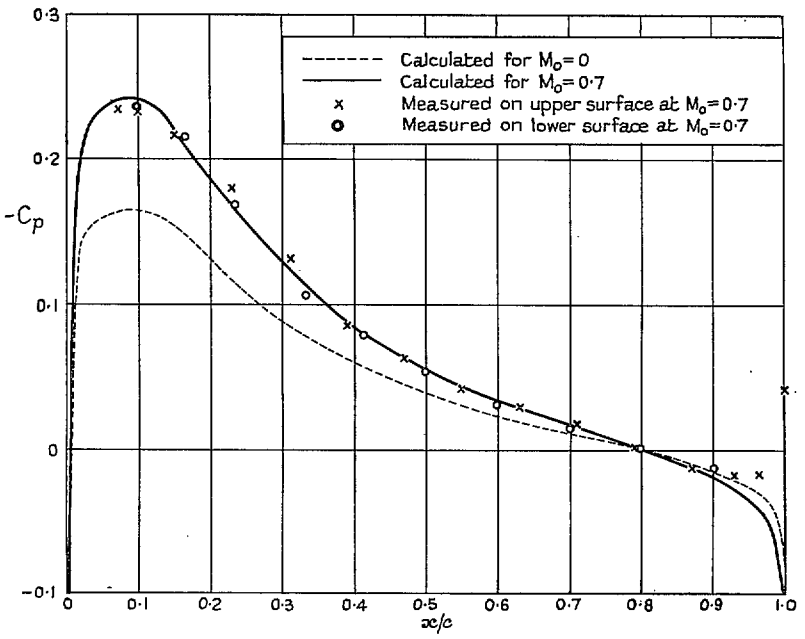

FIG. 5. Calculated and measured pressure distributions for $\alpha = 0$ deg.

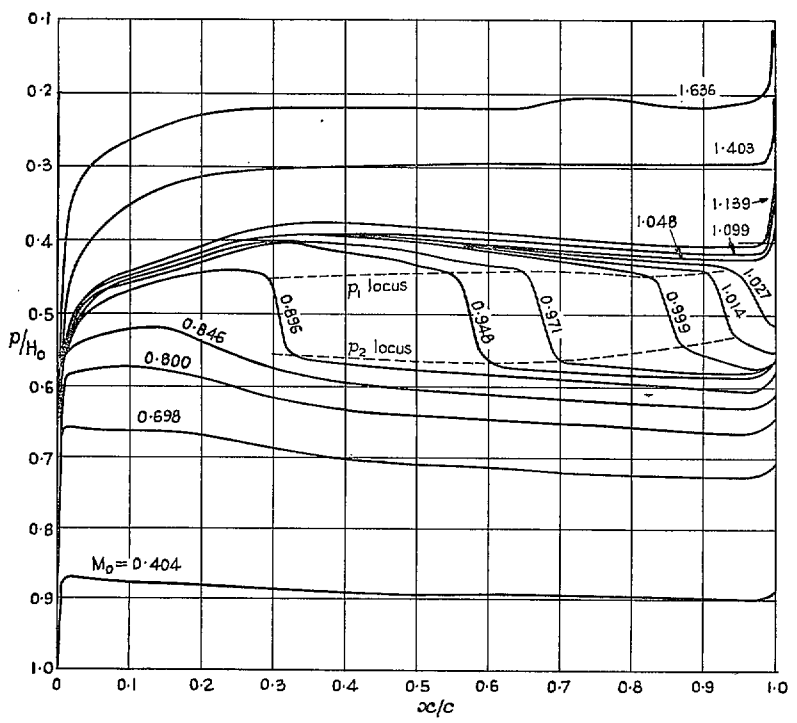

FIG. 6. Pressure distributions for $\alpha = 0$ deg.

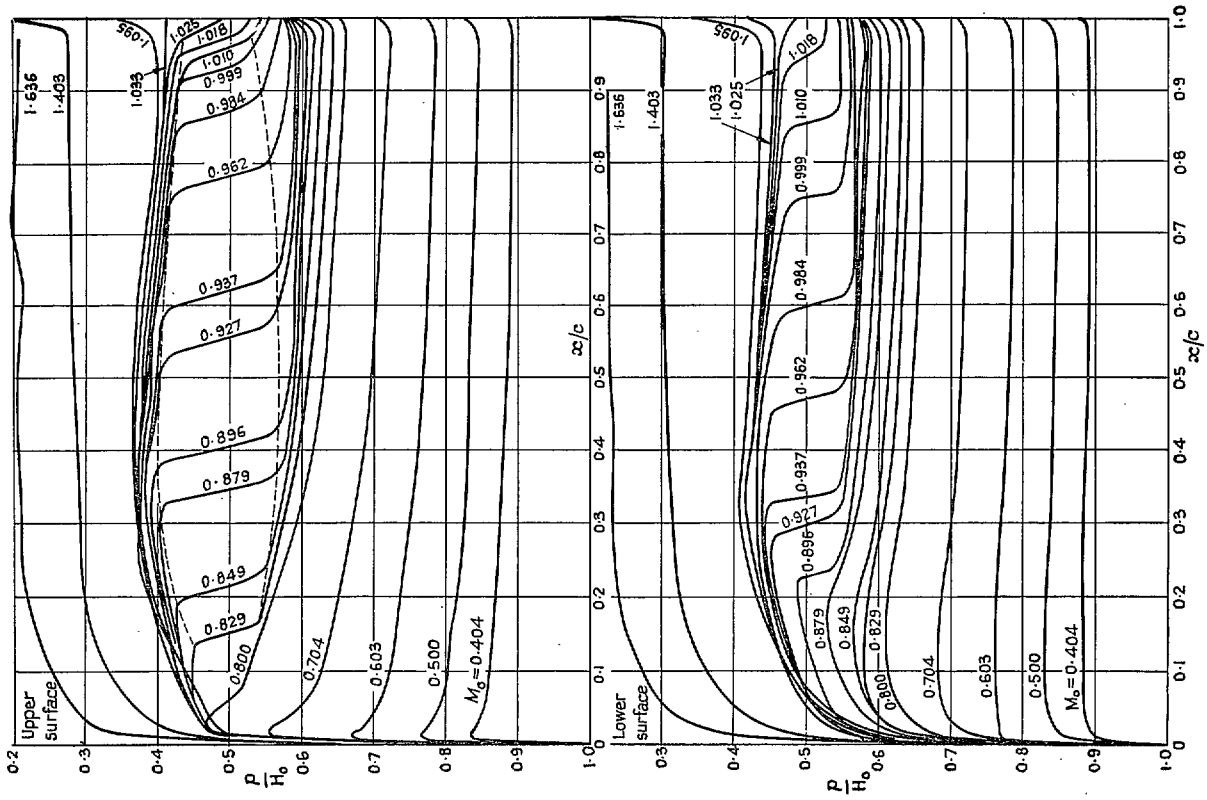

FIG. 7. Pressure distributions for $\alpha = 0{\cdot}5$ deg.

FIG. 8. Pressure distributions for $\alpha = 1$ deg.

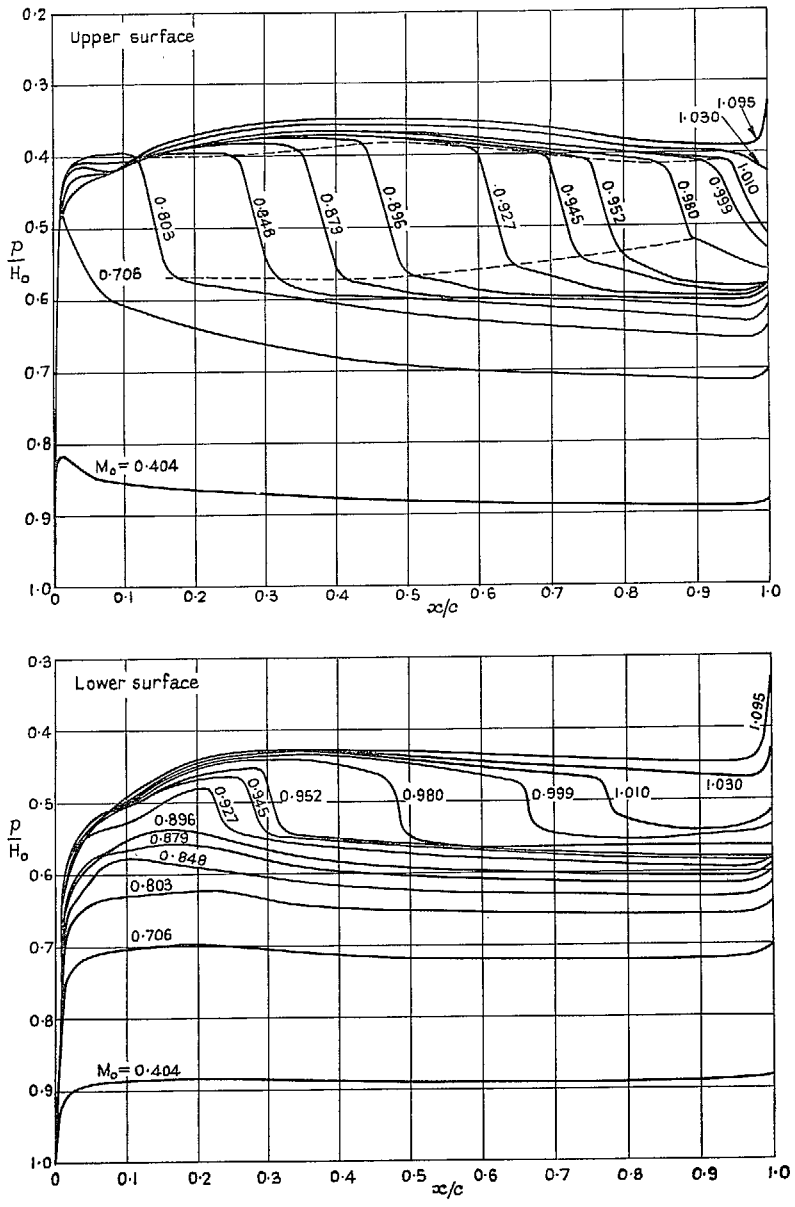

FIG. 9. Pressure distributions for $\alpha = 1 \cdot 5$ deg.

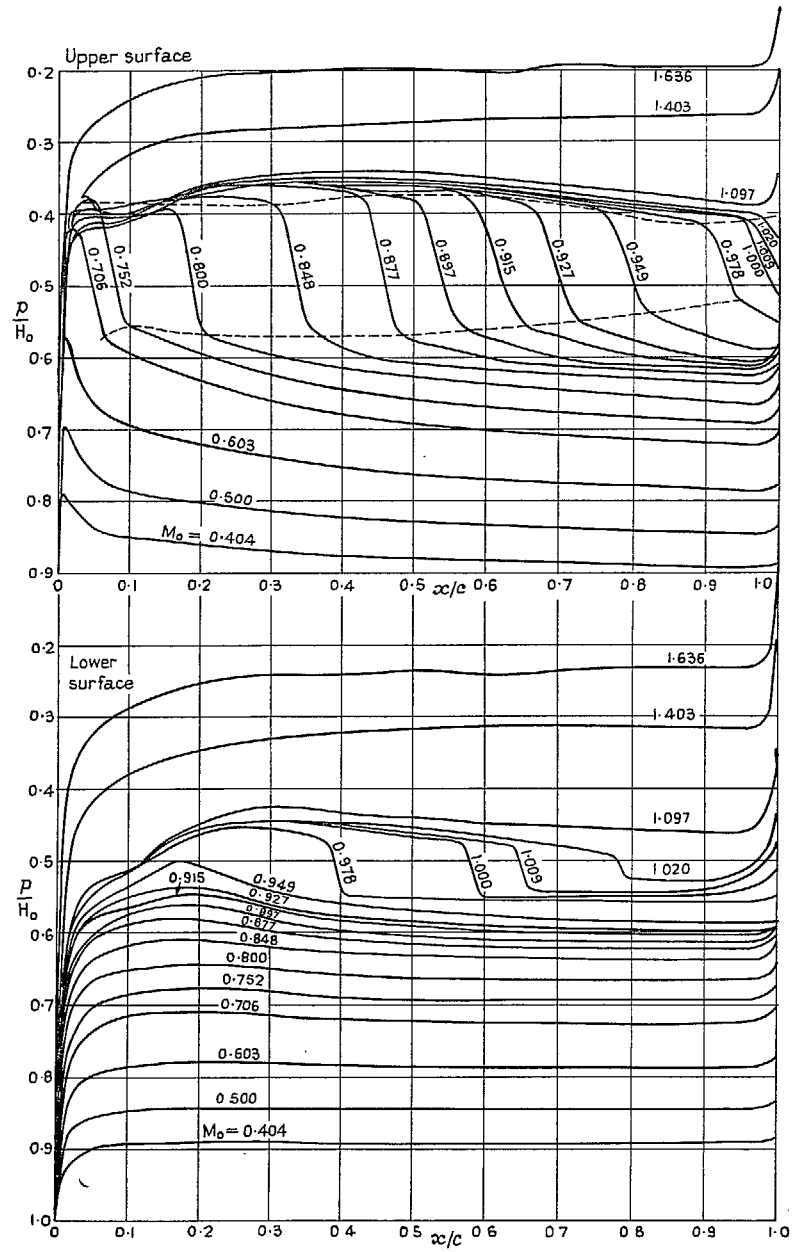

FIG. 10. Pressure distributions for $\alpha = 2$ deg.

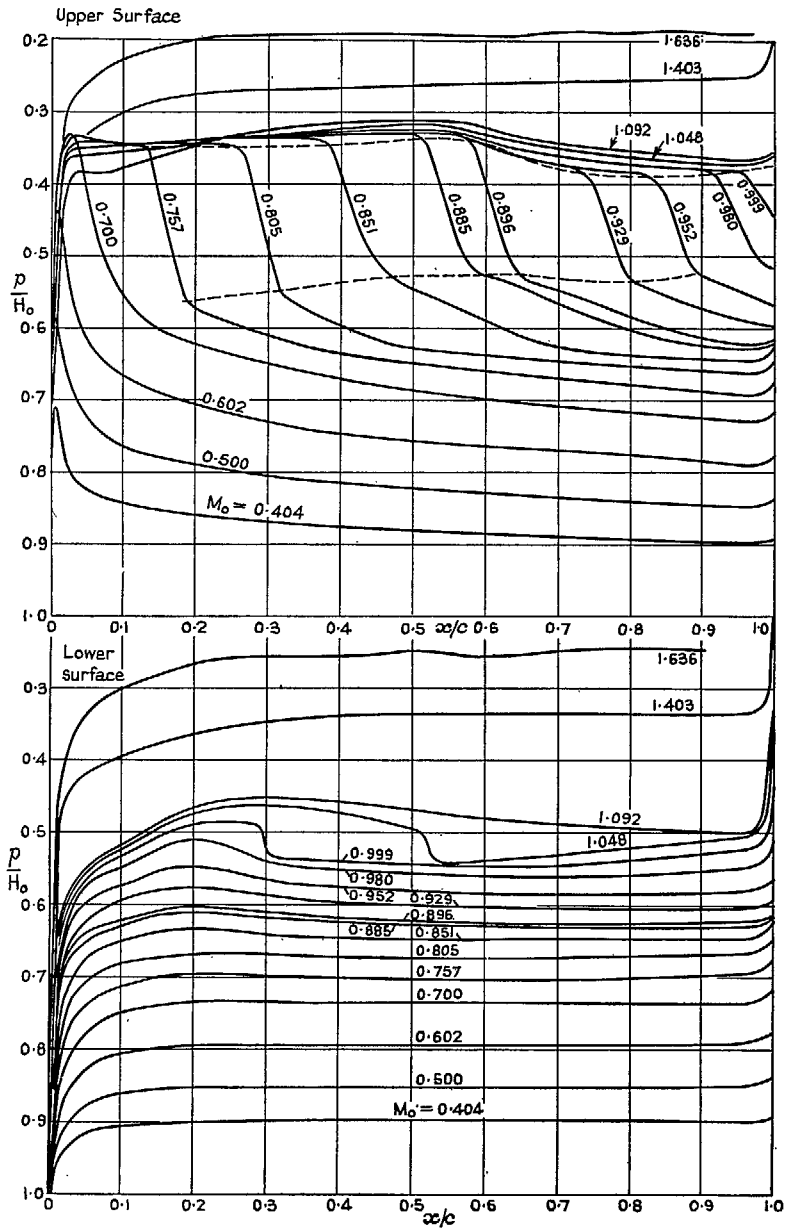

FIG. 11. Pressure distributions for $\alpha = 3$ deg.

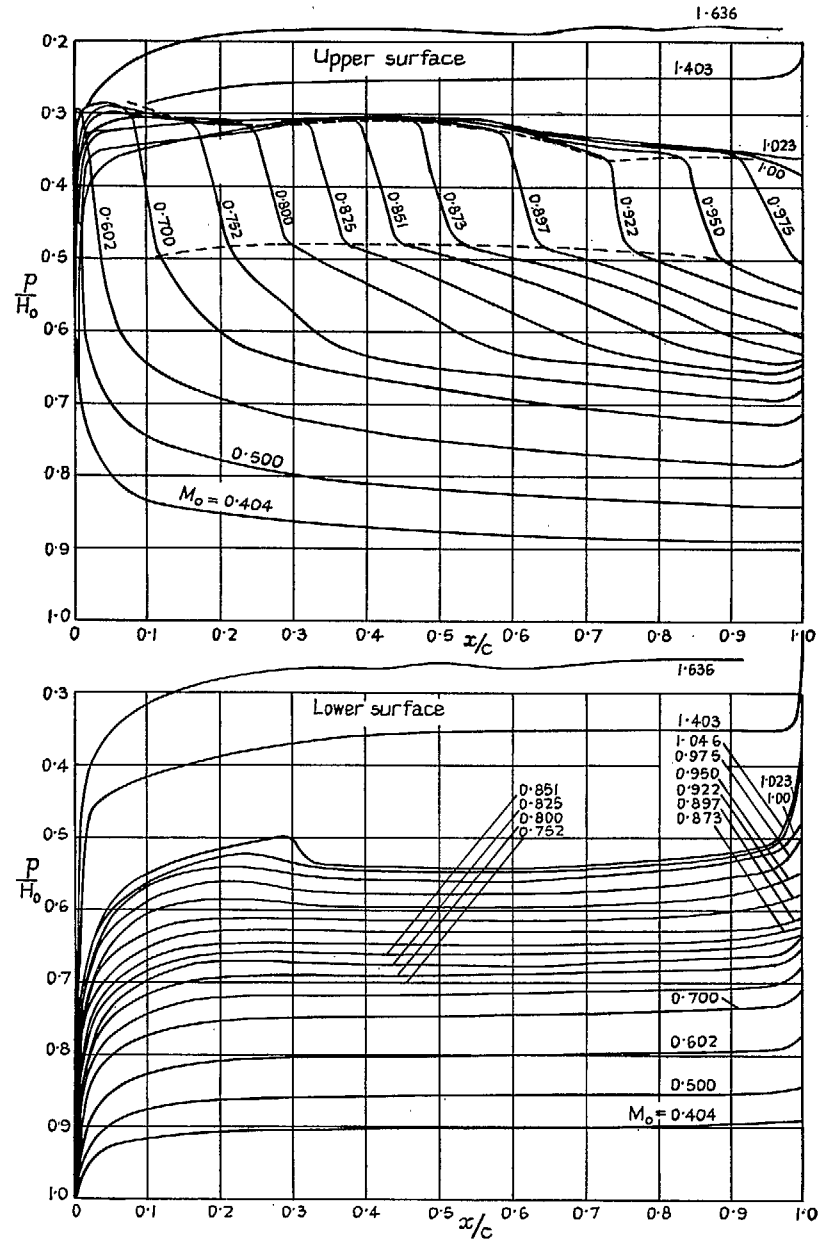

FIG. 12. Pressure distributions for $\alpha = 4$ deg.

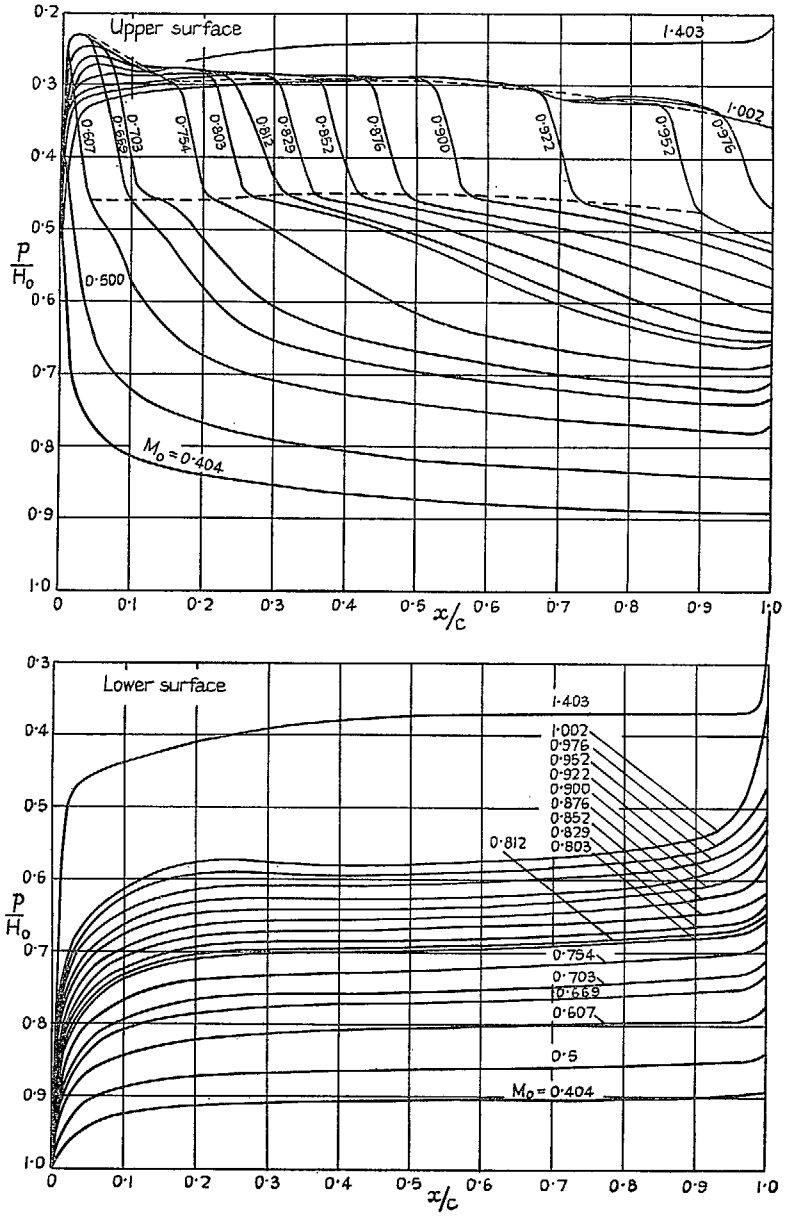

FIG. 13. Pressure distributions for $\alpha = 5$ deg.

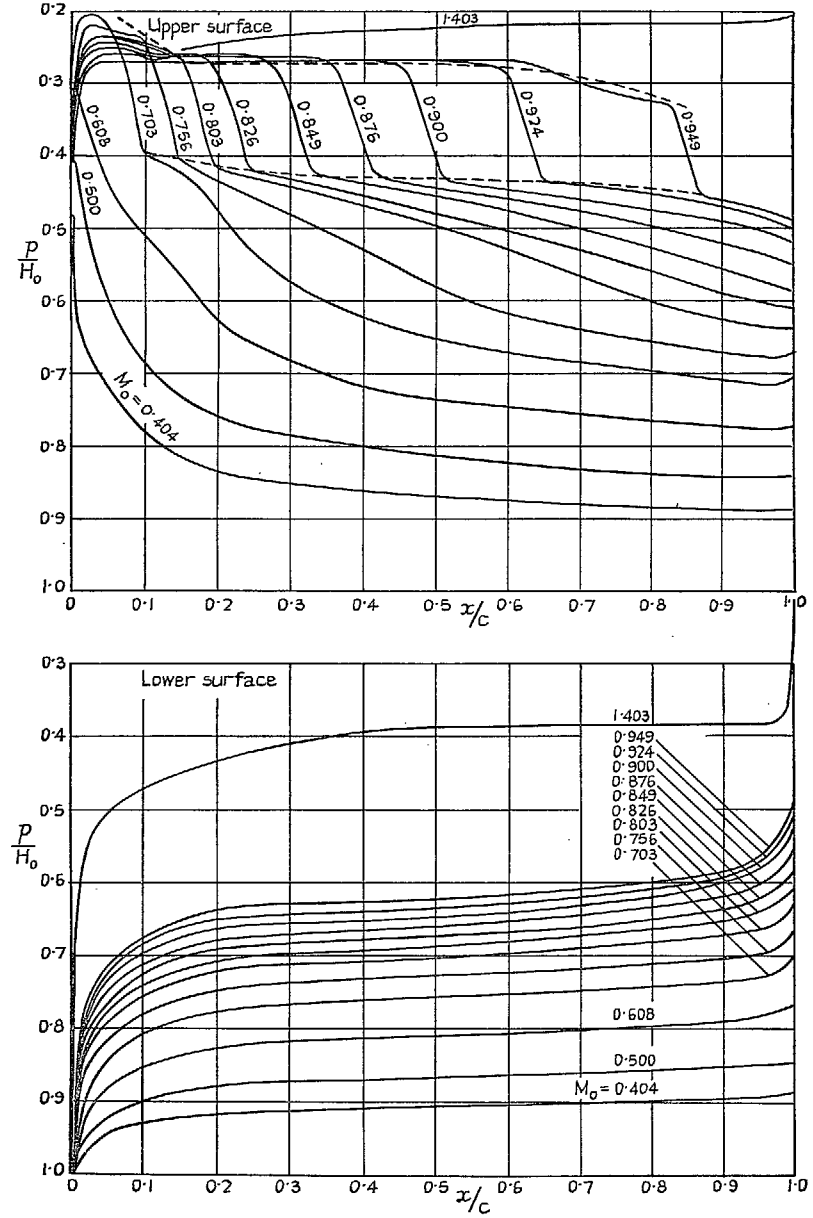

FIG. 14. Pressure distributions for $\alpha = 6$ deg.

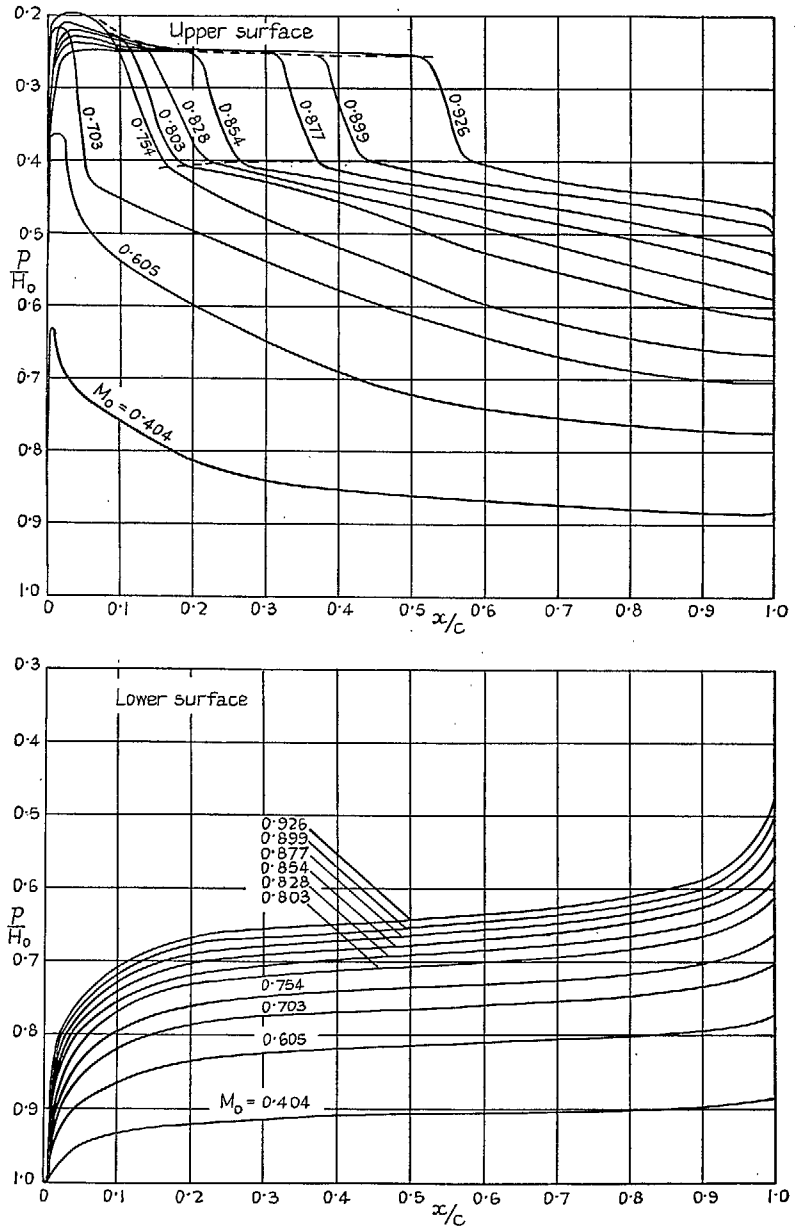

FIG. 15. Pressure distributions for $\alpha = 7$ deg.

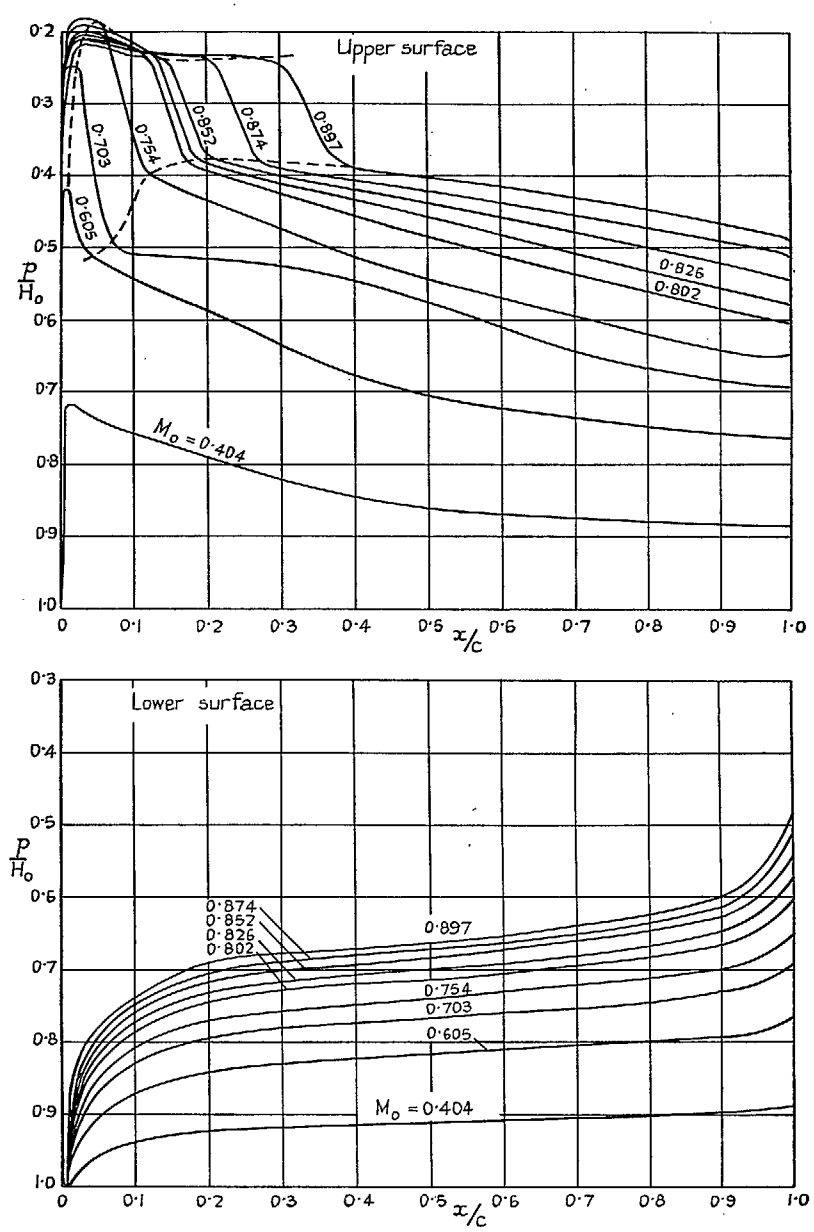

FIG. 16. Pressure distributions for $\alpha = 8$ deg.

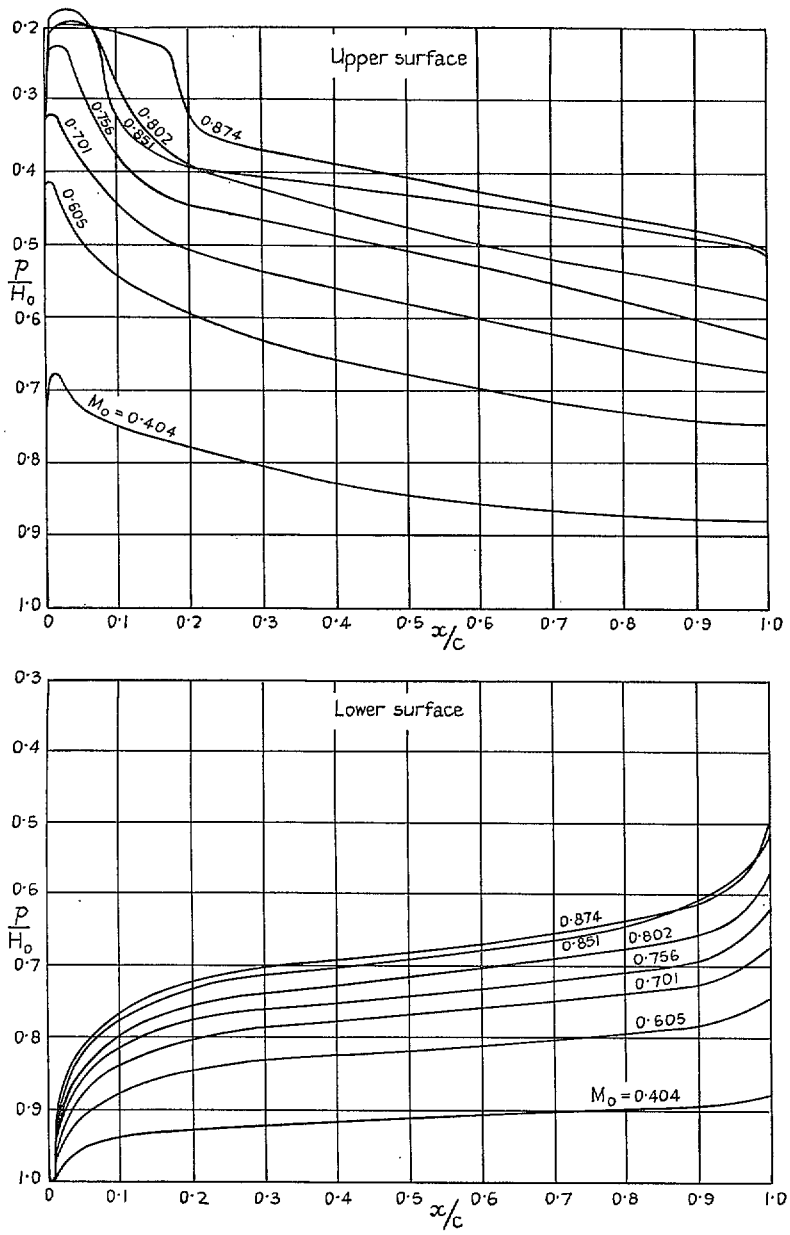

Fig. 17. Pressure distributions for $\alpha = 9$ deg.

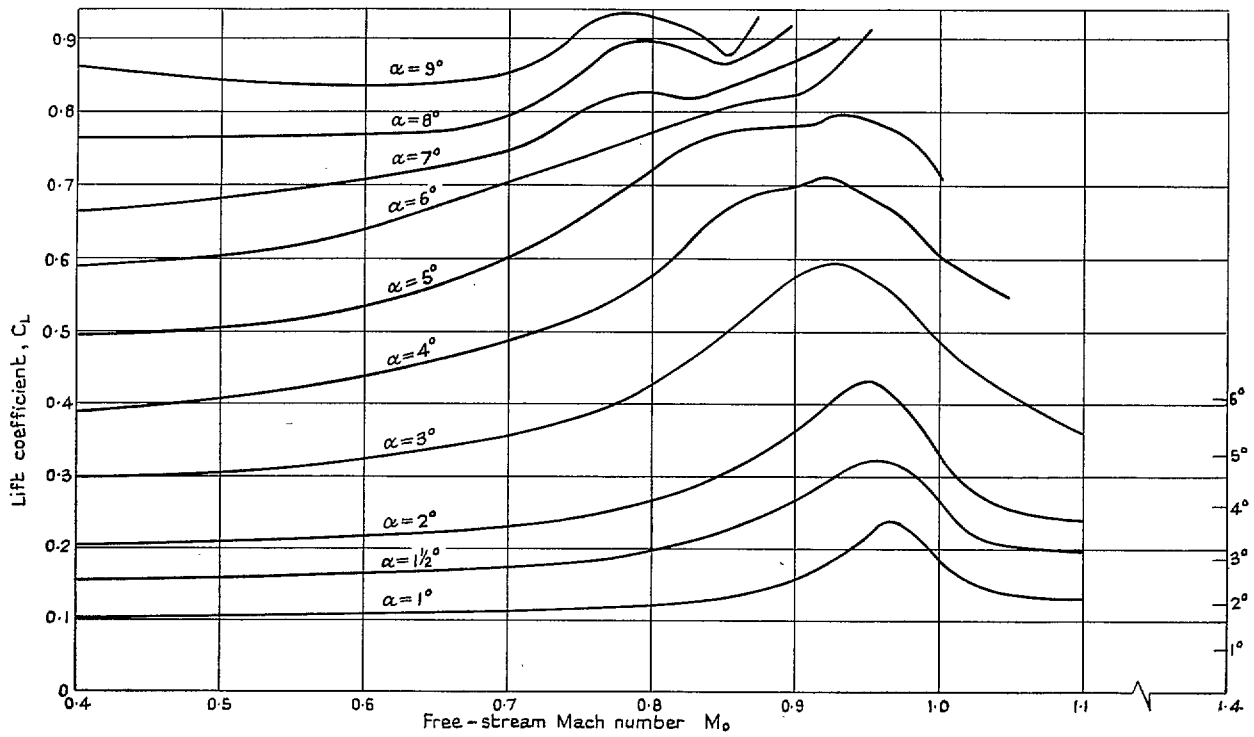

FIG. 18. Variation of lift coefficient with Mach number and incidence.

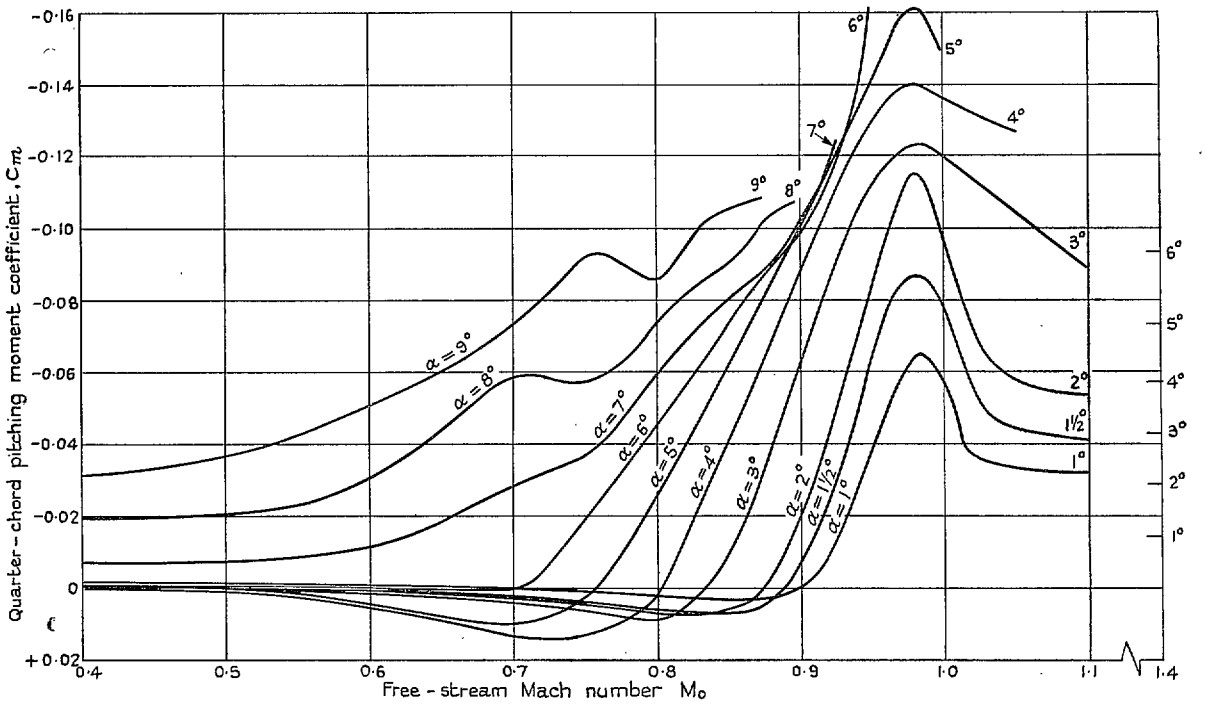

FIG. 19. Variation of pitching-moment coefficient with Mach number and incidence.

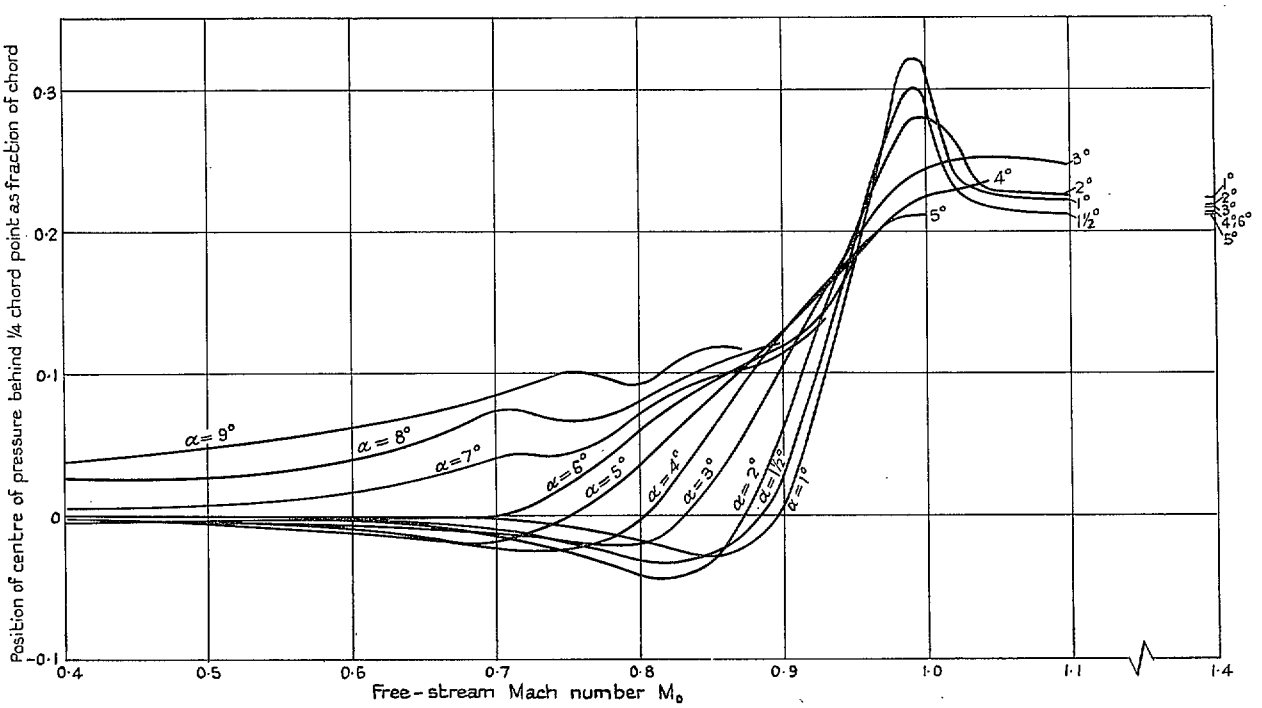

FIG. 20. Variation of centre-of-pressure position with Mach number and incidence.

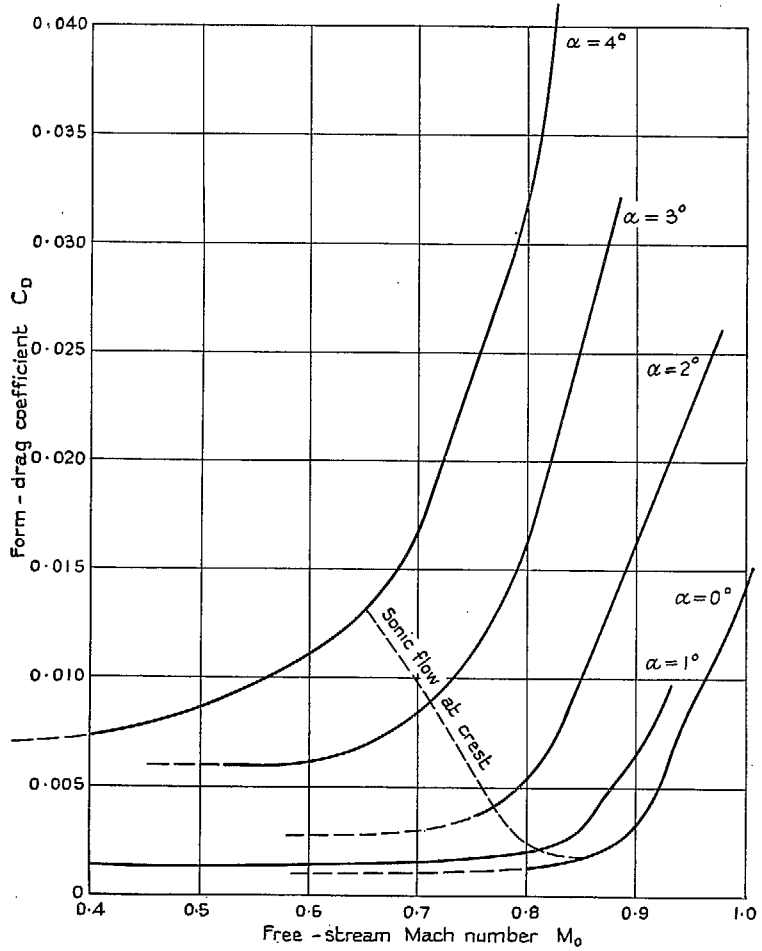

FIG. 21. Variation of form drag coefficient with Mach number and incidence.

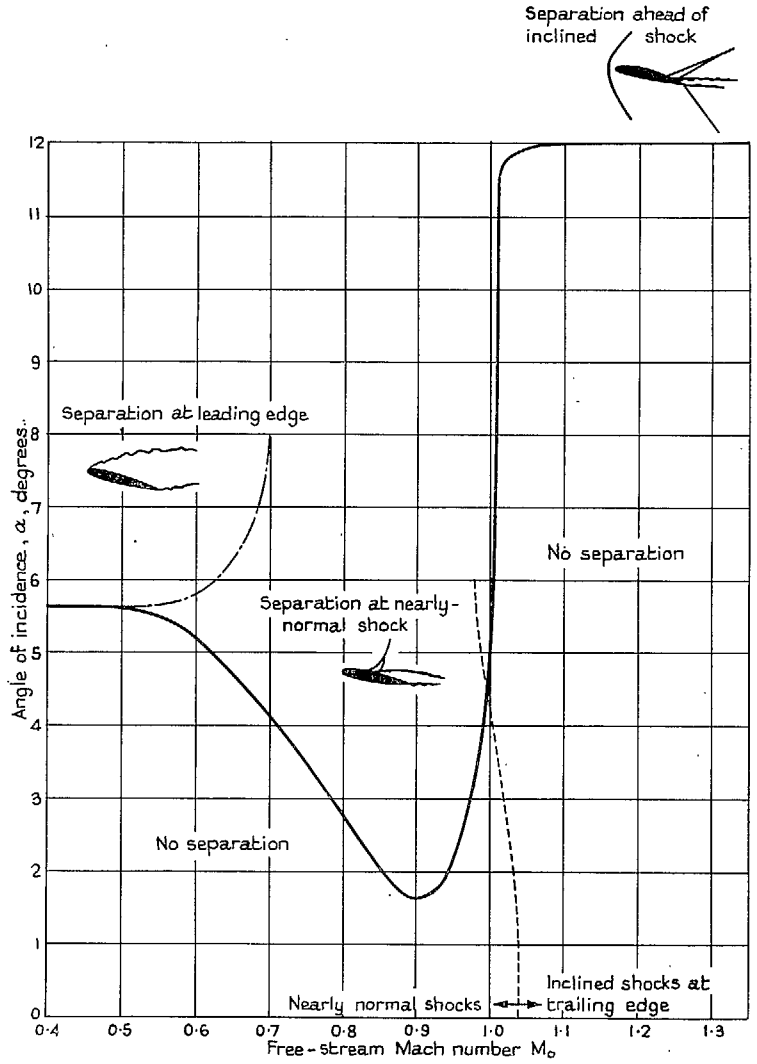

FIG. 22. The types of boundary-layer flow encountered on the aerofoil at different Mach numbers and angles of incidence.

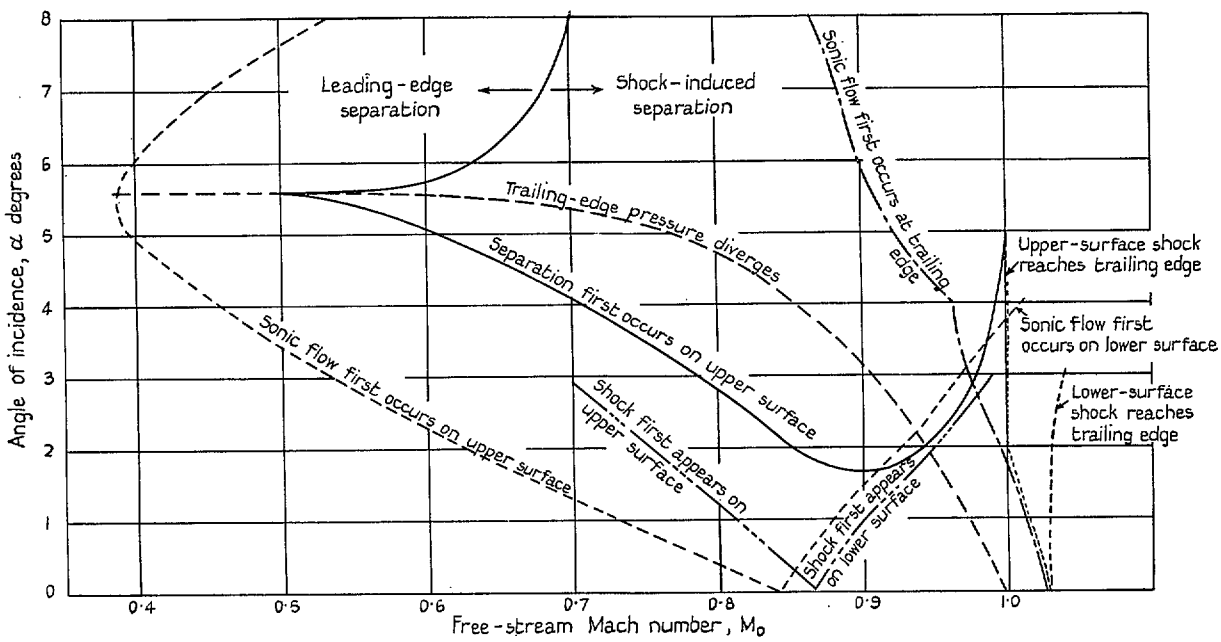

FIG. 23. Values of the Mach number and angle of incidence for the occurrence of various phenomena on the section (NPL 491).

FIG. 24. Schlieren photographs for $\alpha = 1$ deg.

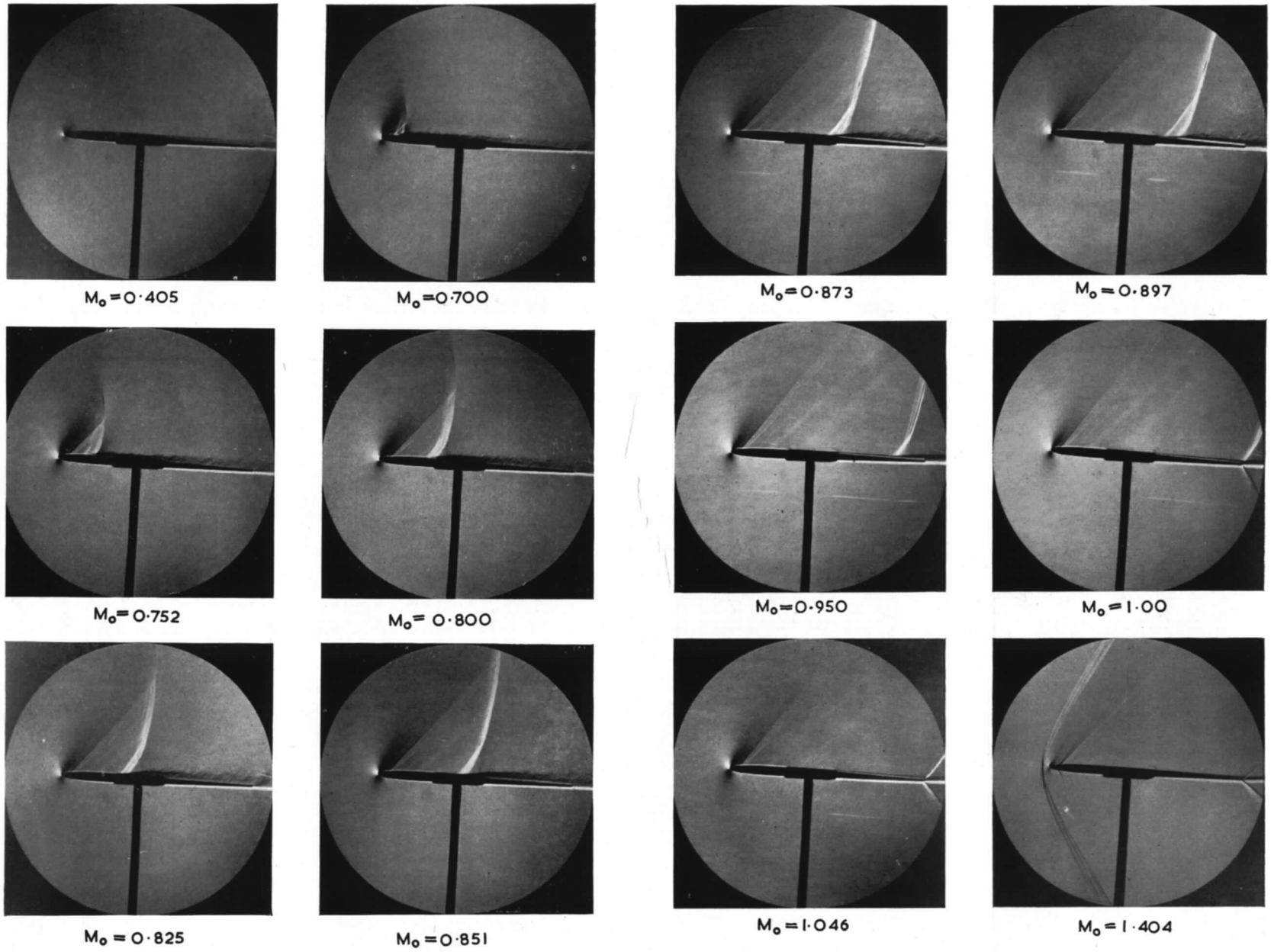

FIG. 25. Schlieren photographs for $\alpha = 4$ deg.

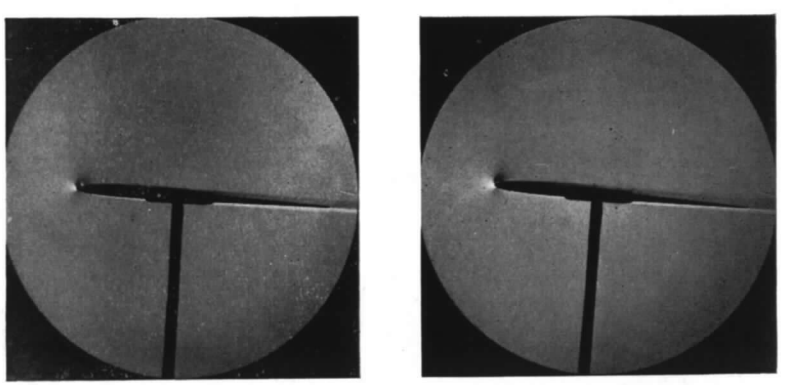

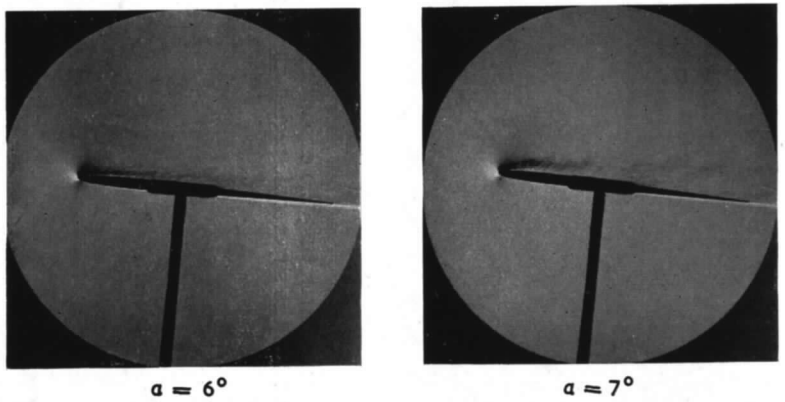

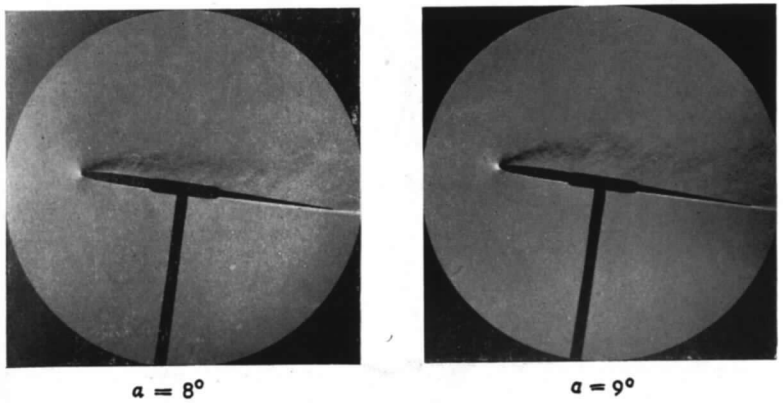

FIG. 26. Schlieren photographs for $M_0 = 0{\cdot}404$.

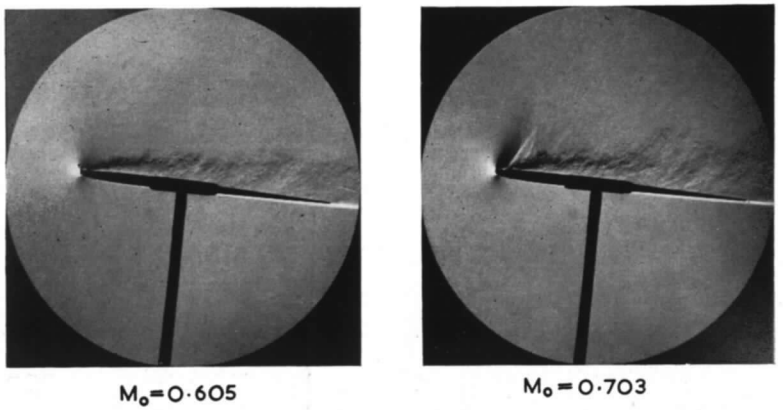

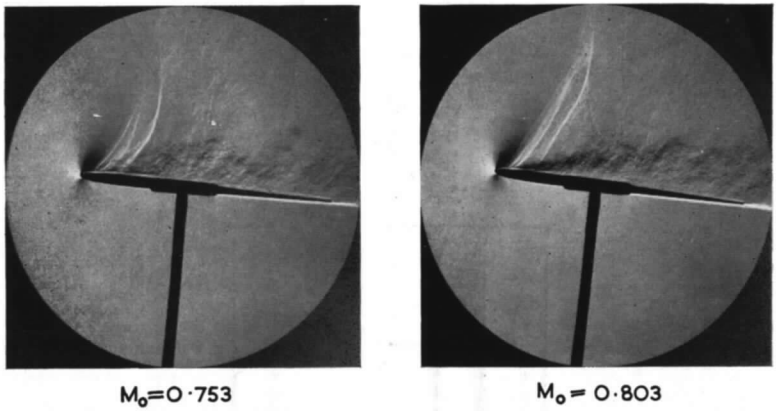

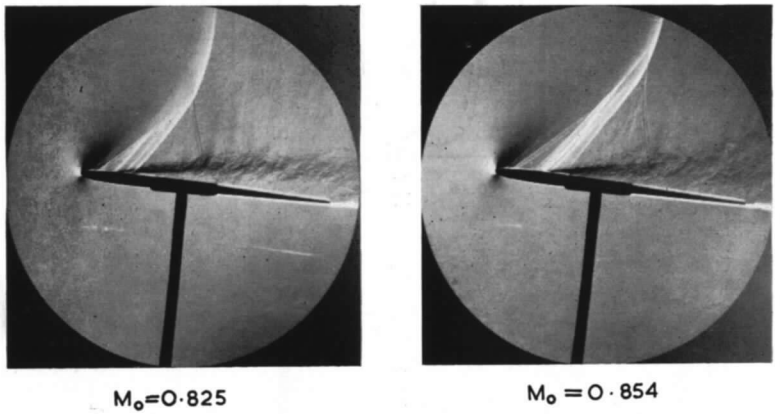

FIG. 27. Schlieren photographs for $\alpha = 7$ deg.

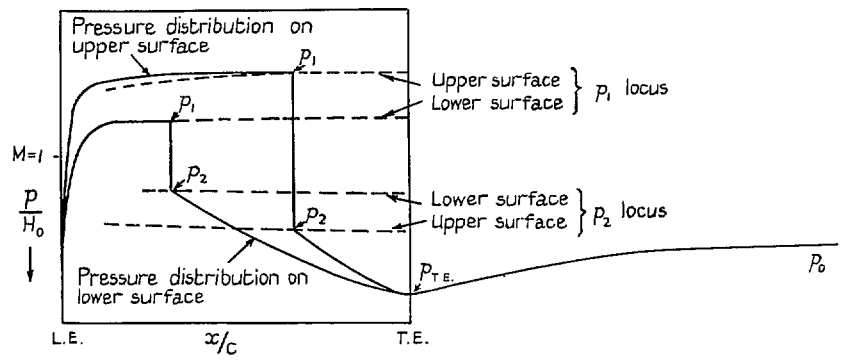

FIG. 28. Sketch illustrating the factors considered in analysing the pressure distributions.

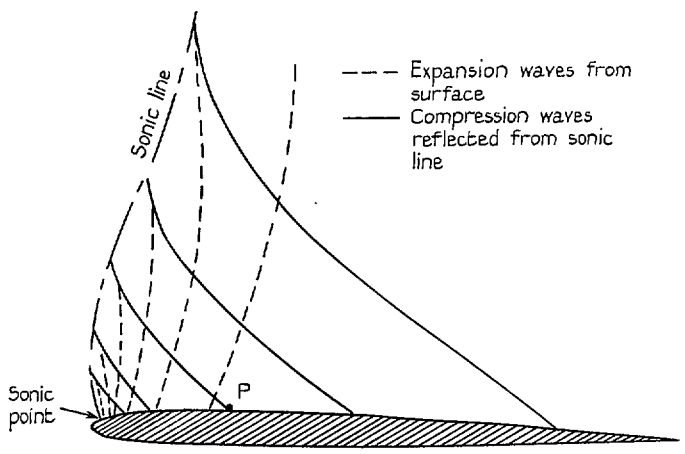

FIG. 29. Sketch illustrating the expansion and compression waves within the supersonic region on an aerofoil.

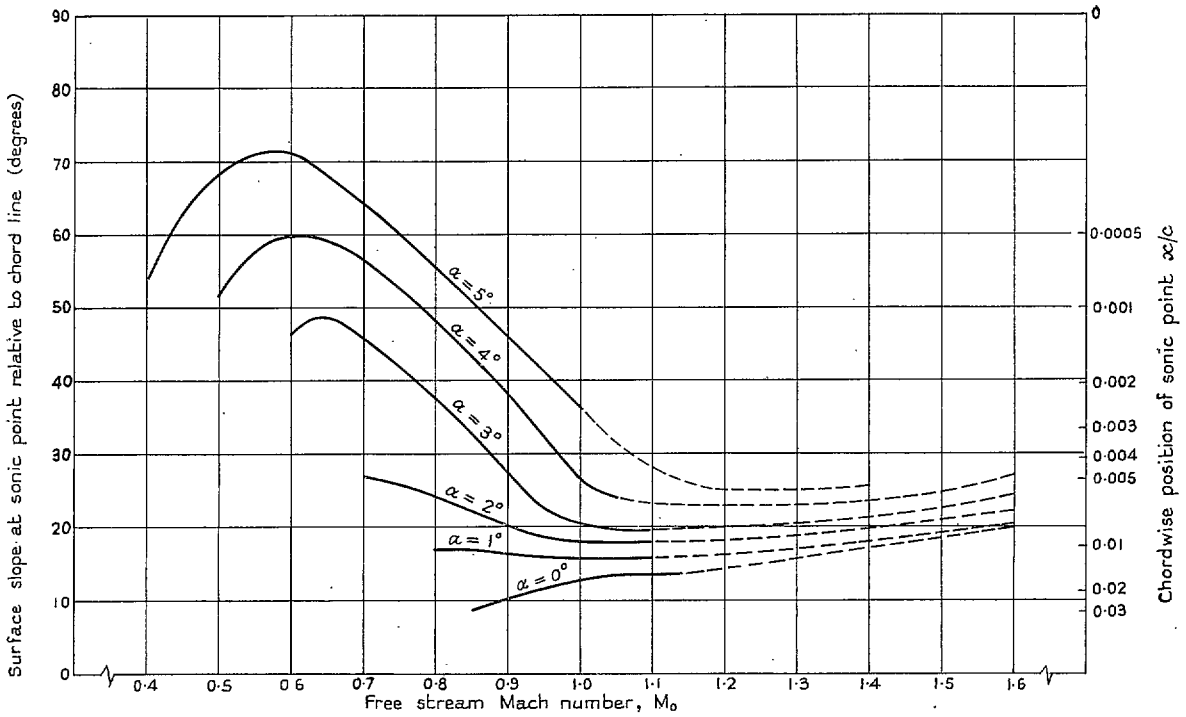

FIG. 30. Variation with Mach number and incidence of the sonic-point position on the upper surface.

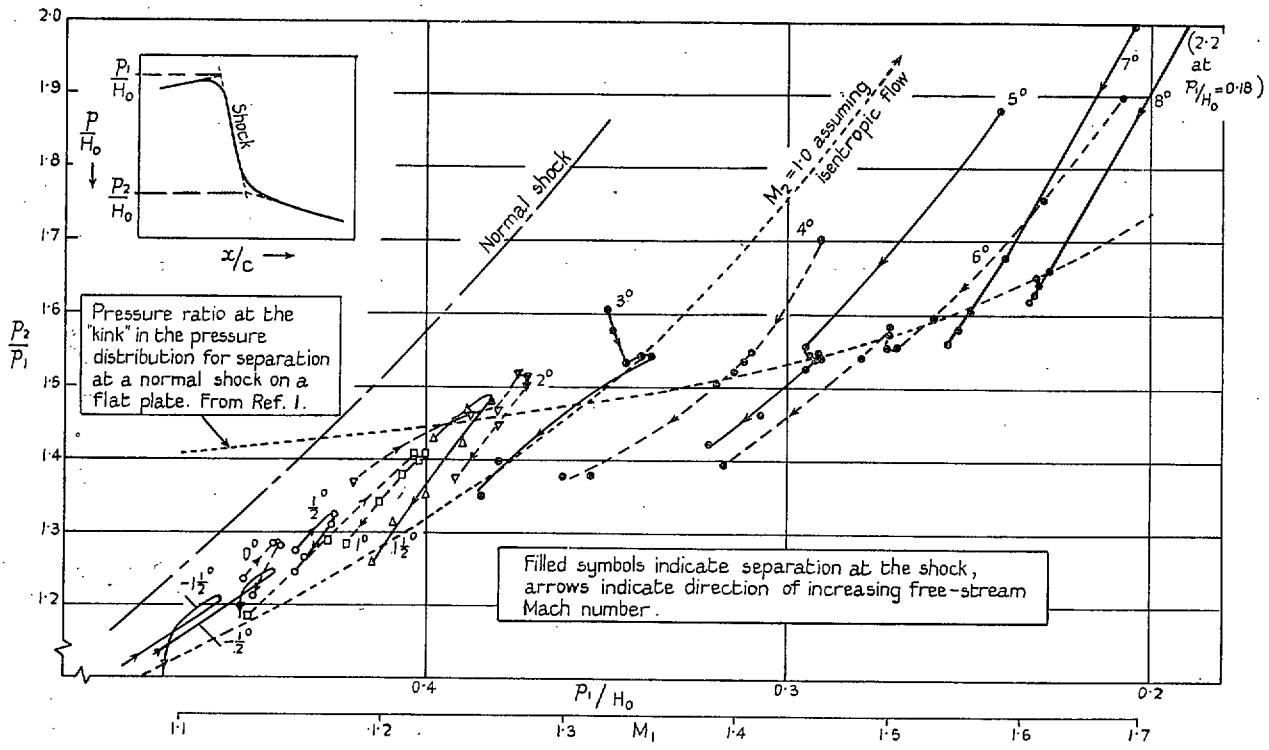

FIG. 31. Pressure ratio across the shock on the upper surface for a range of angle of incidence.

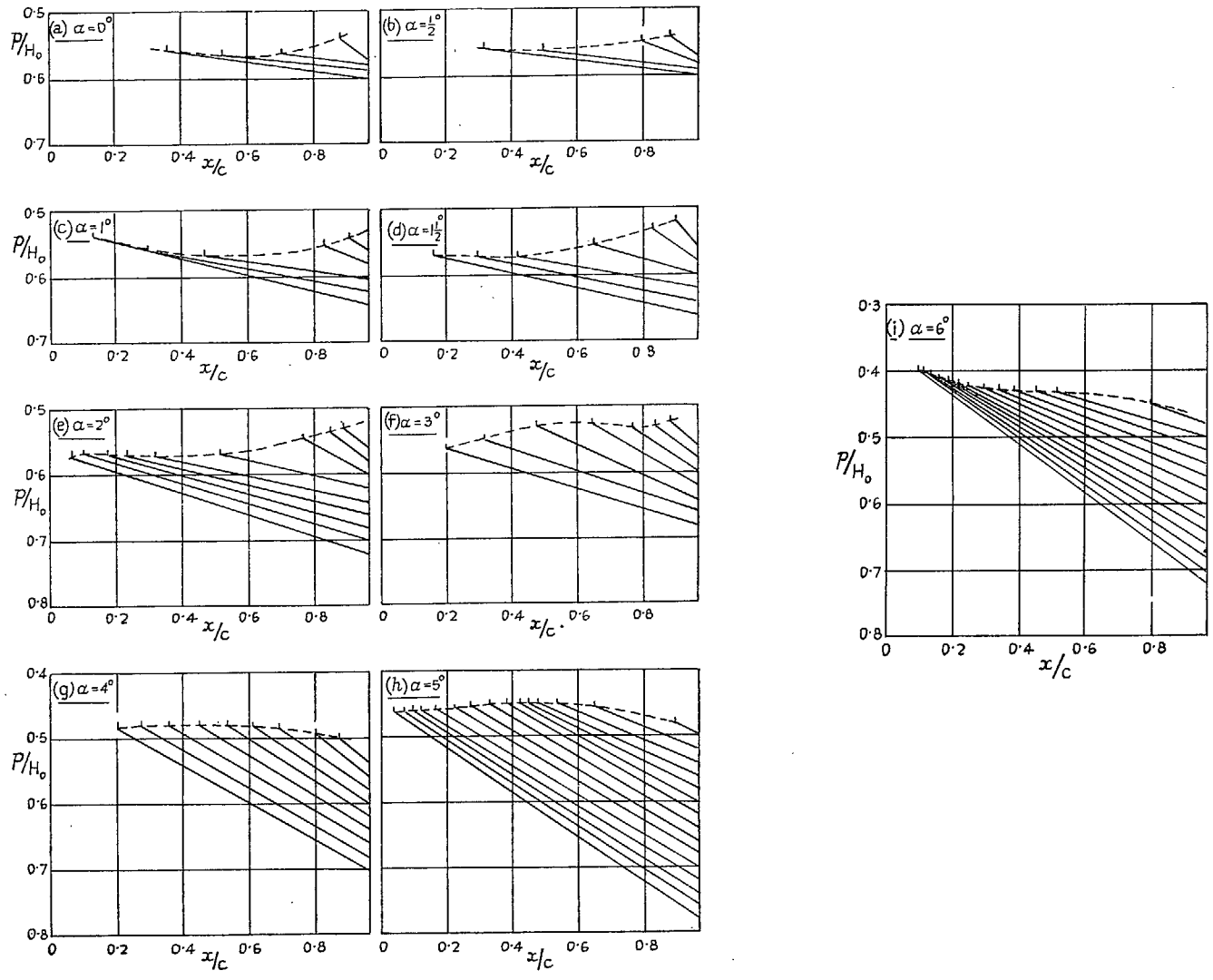

FIGS. 32a to 32i. The p_2 loci and the average pressure gradients between the shock and 0·965 chord on the upper surface.

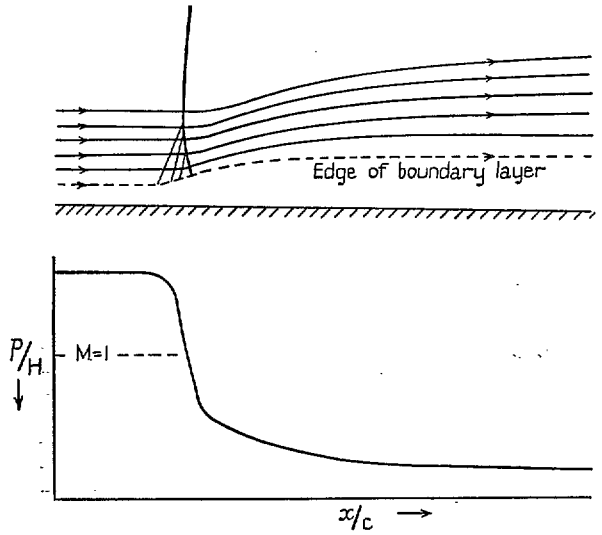

FIG 33. Sketch of flow pattern and surface pressure distribution when the shock is too weak to provoke separation.

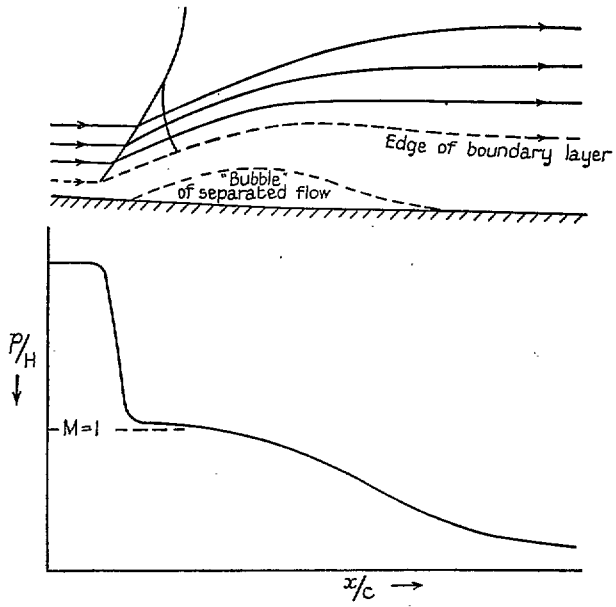

FIG. 34. Sketch of flow pattern and surface-pressure distribution when the shock is strong enough to provoke separation.

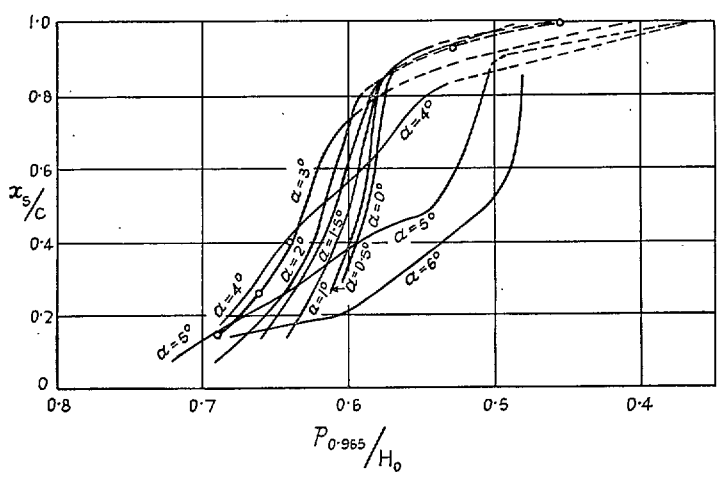

FIG. 35. Variation of the chordwise position of the upper-surface shock with the pressure at 0·965 chord on the upper surface (the curves are shown broken when $p_{0·965}$ is influenced by the proximity of the shock).

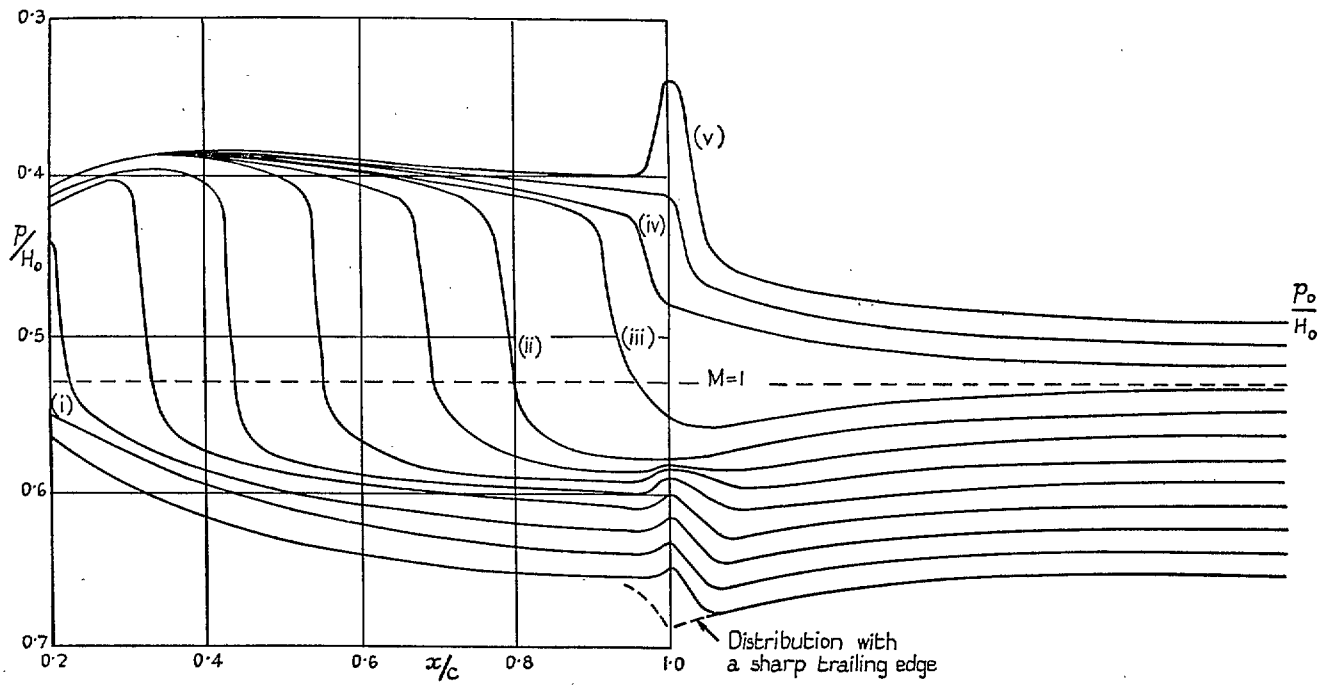

FIG. 36. Sketches of the pressure distributions along the upper surface and wake for $\alpha = 1$ deg.

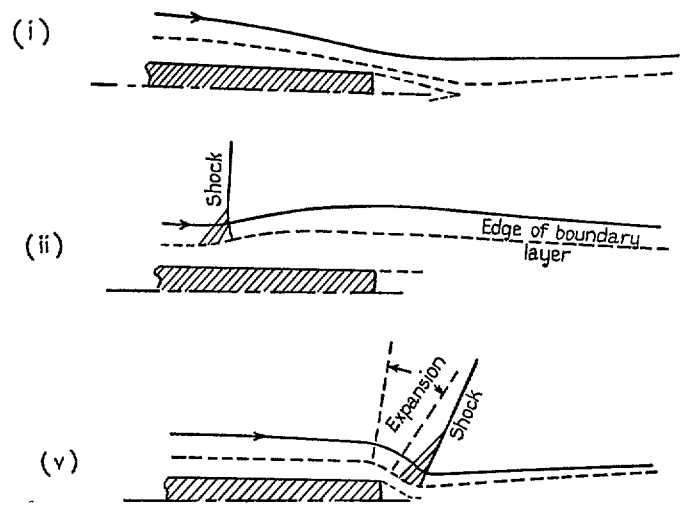

FIG. 37. Sketches of the flow pattern on the upper surface near the trailing edge for $\alpha = 1$ deg (the numbers on the diagrams refer to Fig. 36).

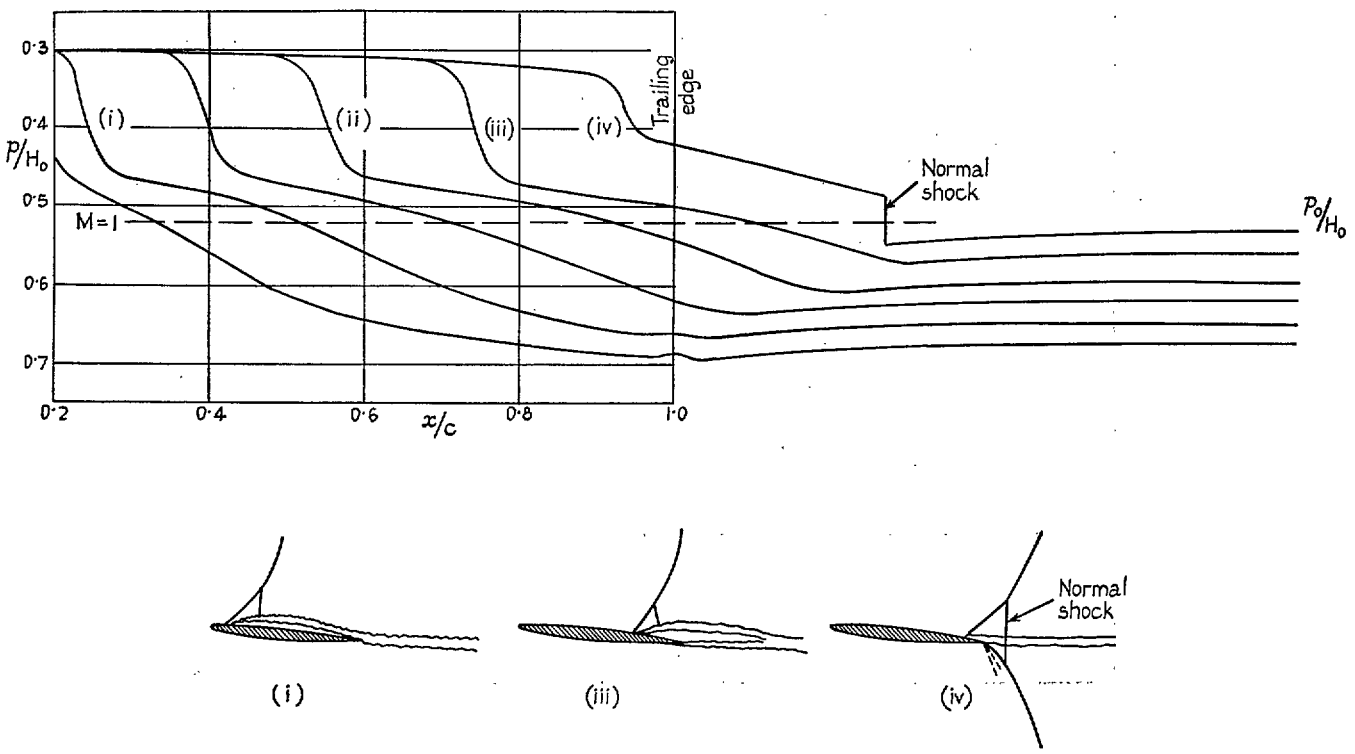

FIG. 38. Sketches of the pressure distributions along the upper surface and wake for $\alpha = 5$ deg.

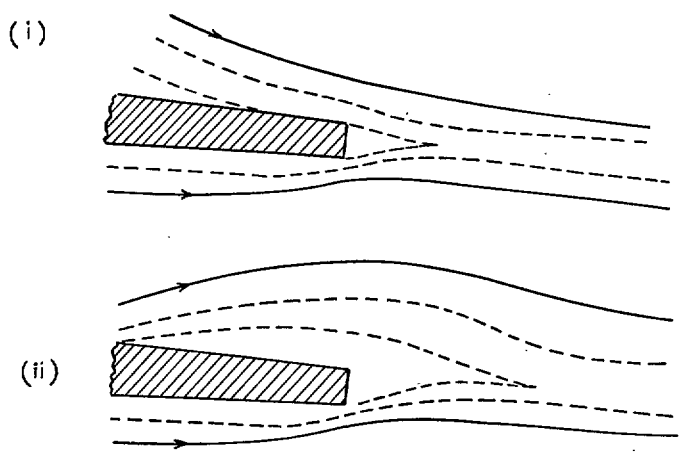

FIG. 39. Sketches of the flow pattern near the trailing edge for $\alpha = 5$ deg (the numbers on the diagrams refer to Fig. 38).

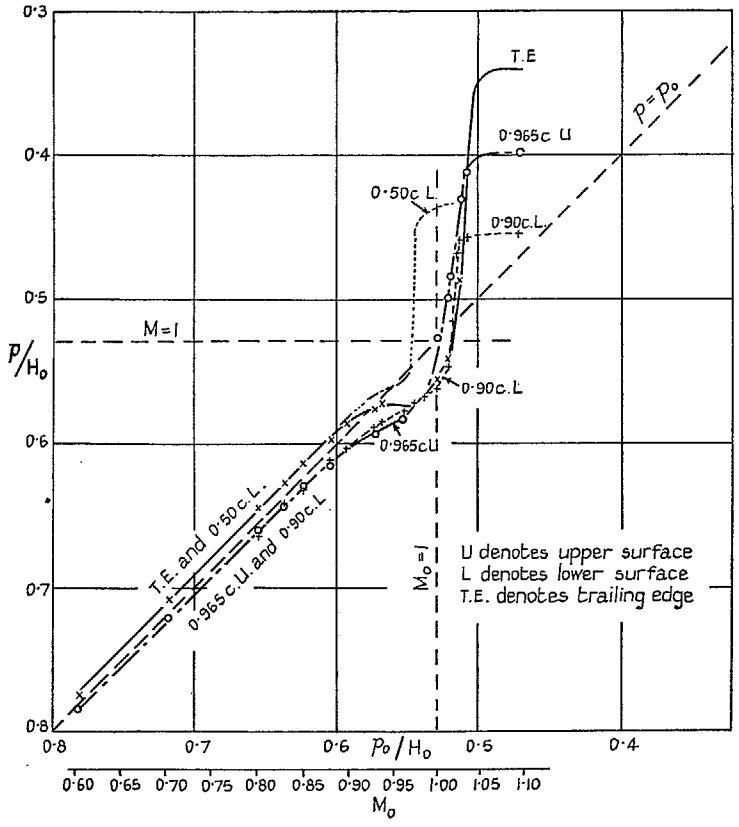

FIG. 40. The variation with free-stream pressure of the pressures at various points on the surface ($\alpha = 1$ deg).

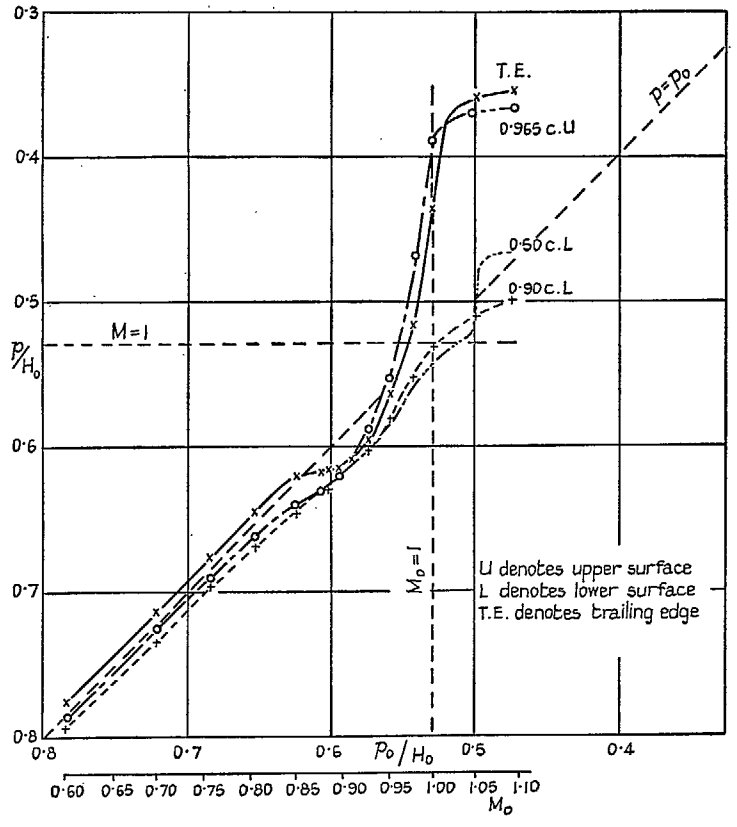

FIG. 41. The variation with free-stream pressure of the pressures at various points on the surface ($\alpha = 3$ deg).

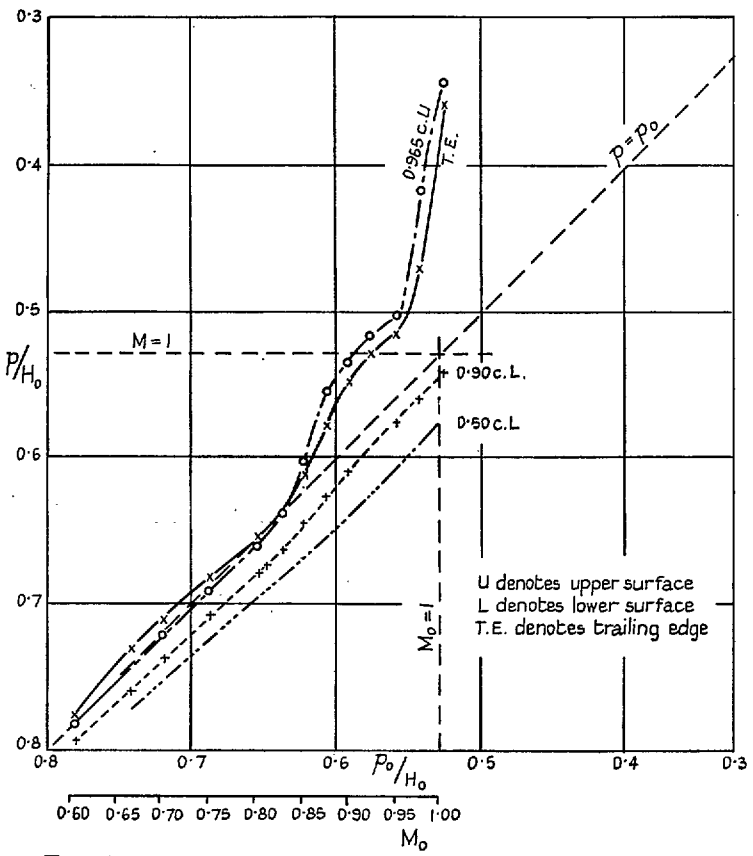

FIG. 42. The variation with free-stream pressure of the pressures at various points on the surface ($\alpha = 5$ deg).

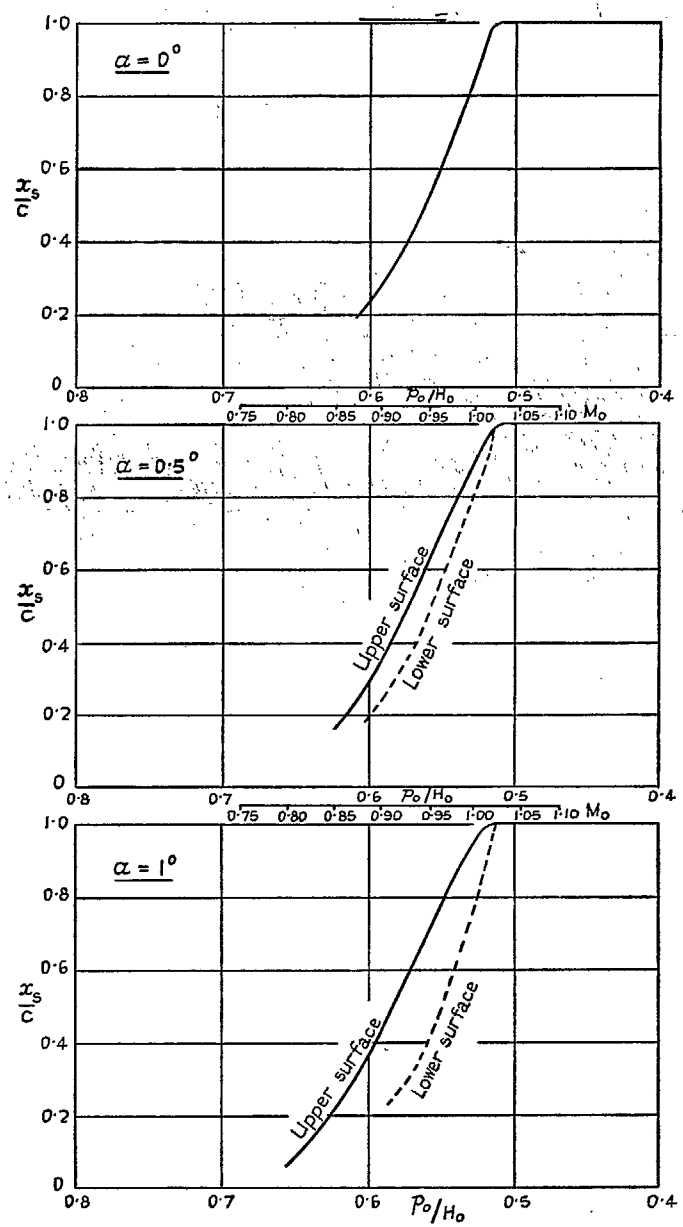

FIG 43a. Variation of shock-wave position with free-stream pressure.

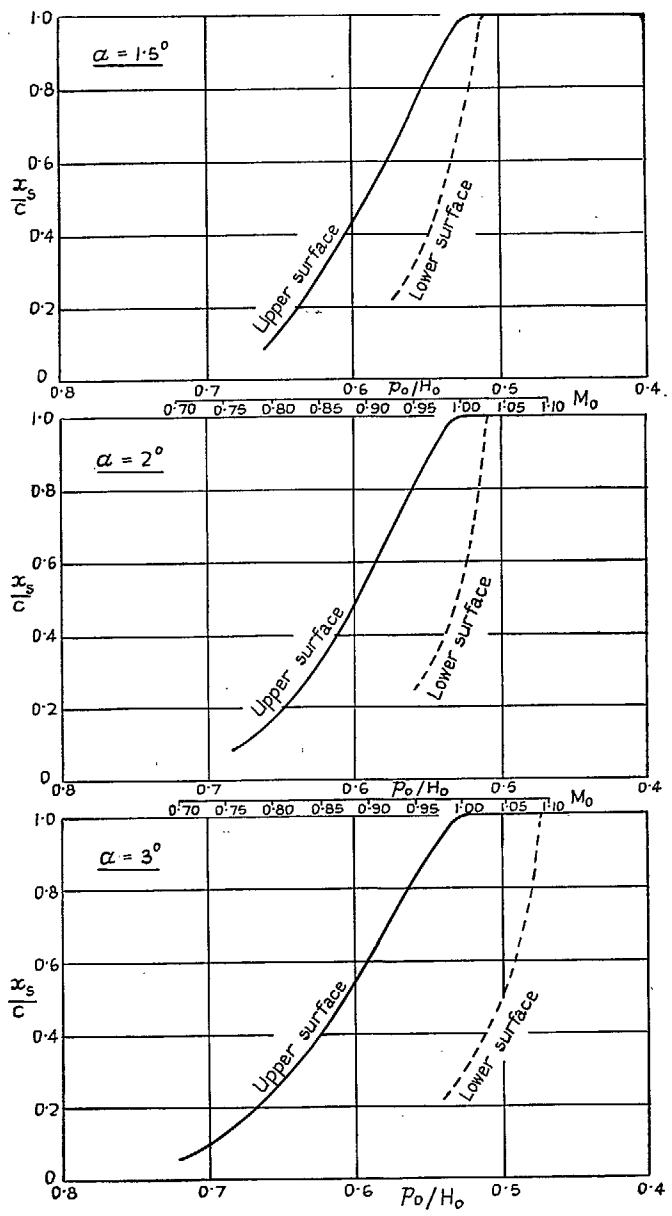

FIG. 43b. Variation of shock-wave position with free-stream pressure.

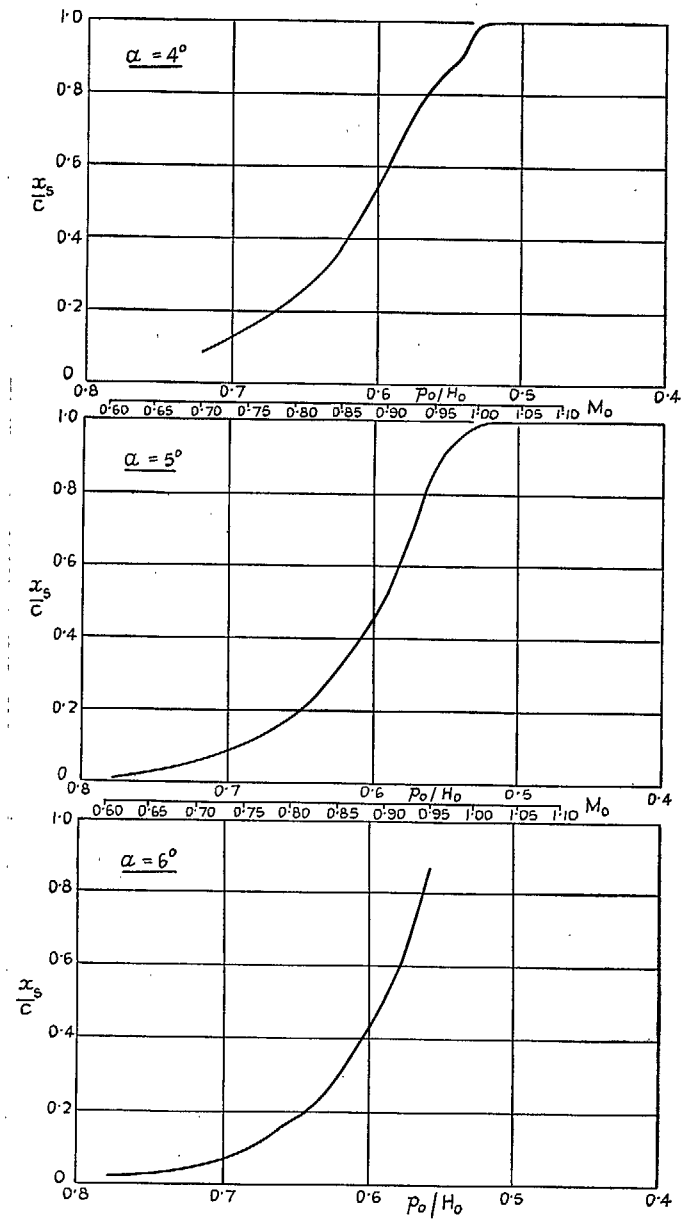

FIG. 43c. Variation of shock-wave position with free-stream pressure.

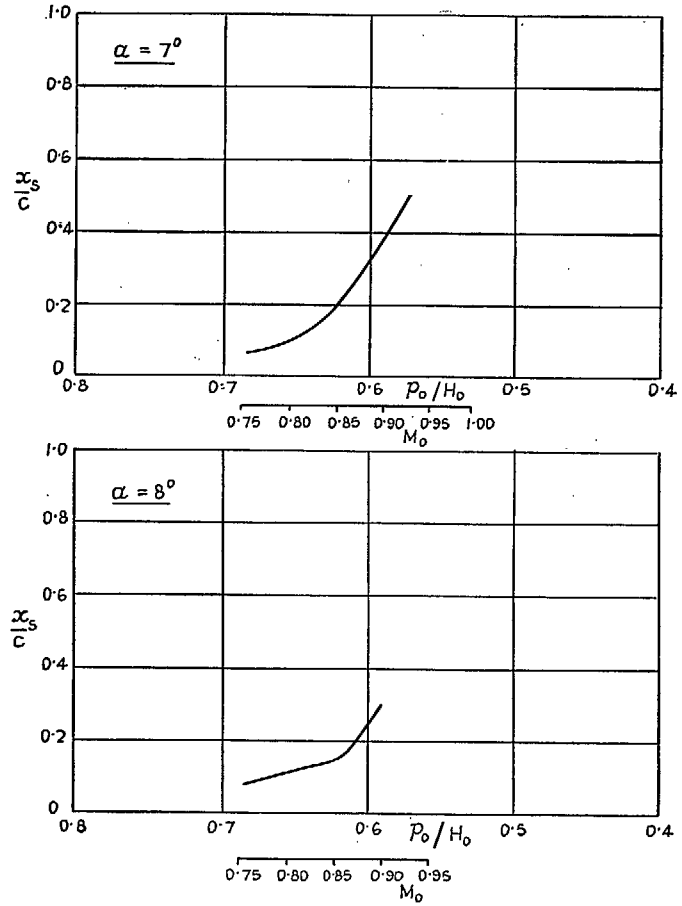

FIG. 43d. Variation of shock-wave position with free-stream pressure.

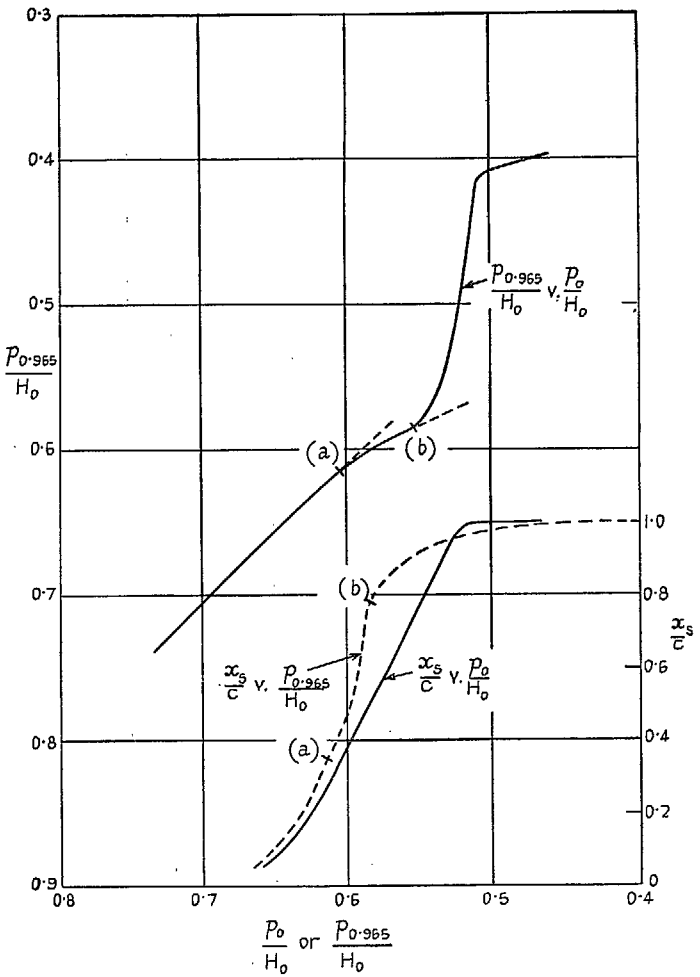

FIG. 44a. The variation of free-stream pressure and upper-surface shock position with the pressure at 0·965 chord on the upper surface ($\alpha = 1$ deg).

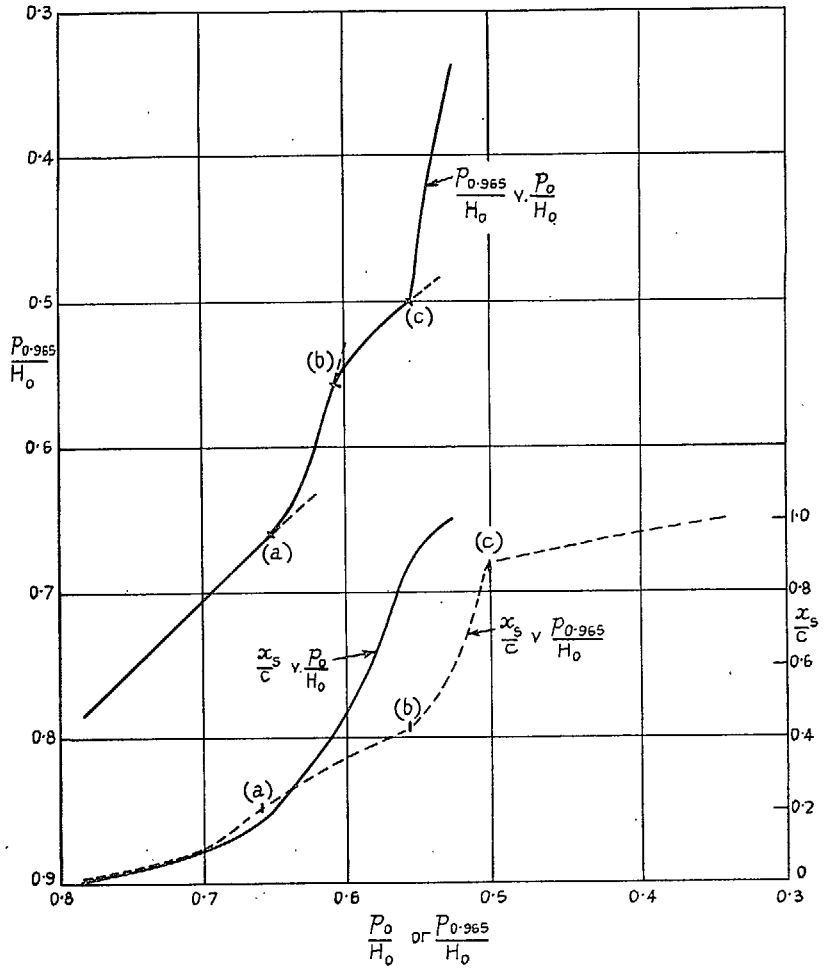

FIG. 44b. The variation of free-stream pressure and upper-surface shock position with the pressure at 0·965 chord on the upper surface ($\alpha = 5$ deg).

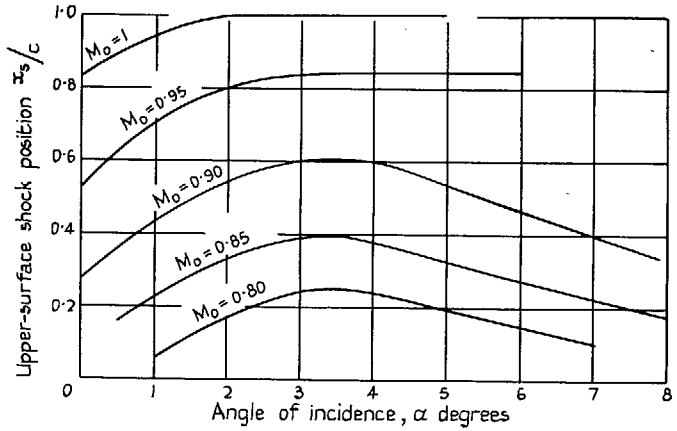

FIG. 45. Variation of the upper-surface shock position with angle of incidence.

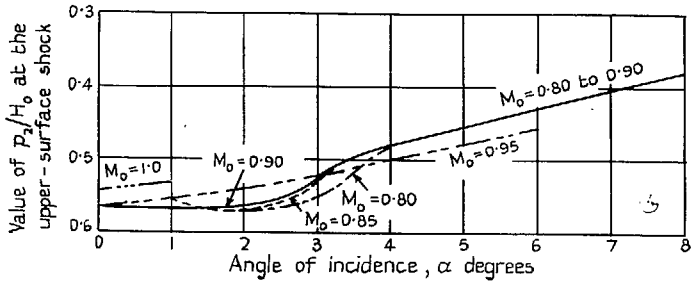

FIG. 46. Variation of the pressure p_2 immediately downstream of the upper-surface shock with angle of incidence.

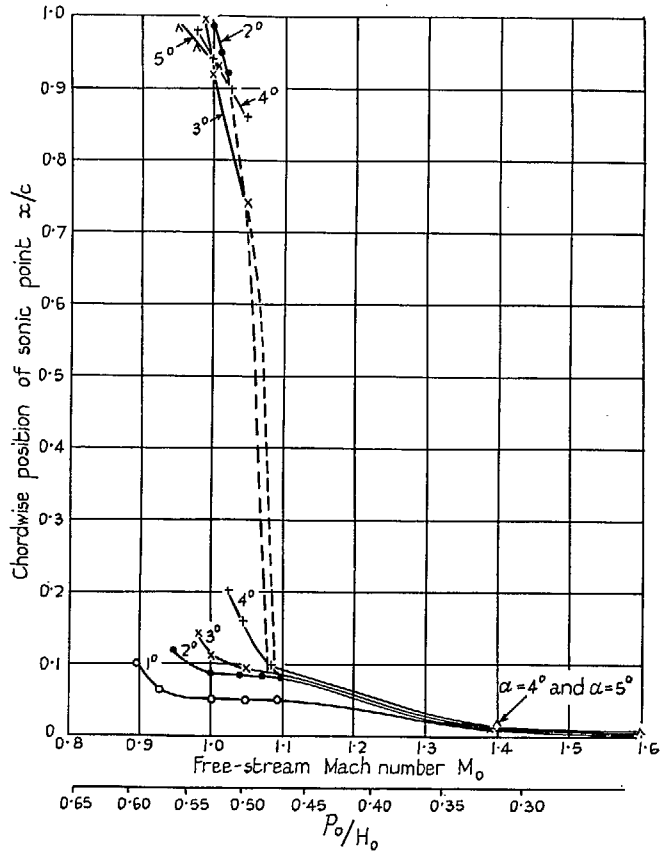

FIG. 47. Variation of the sonic-point positions on the lower surface with Mach number and incidence.

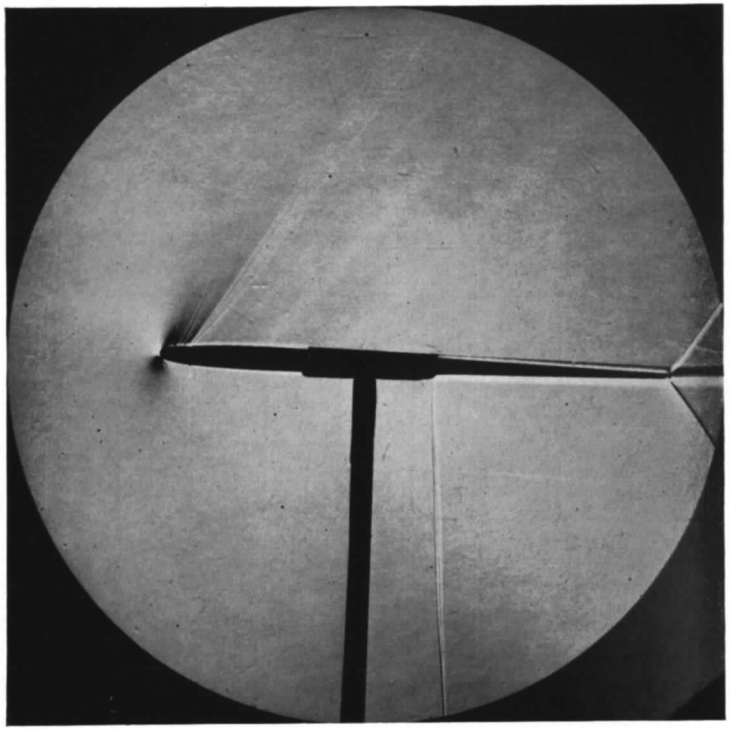

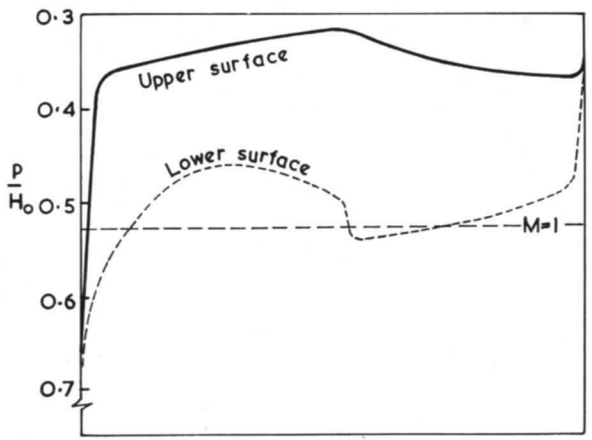

FIG. 48. The flow at $M_0 = 1{\cdot}048$, $\alpha = 3$ deg.

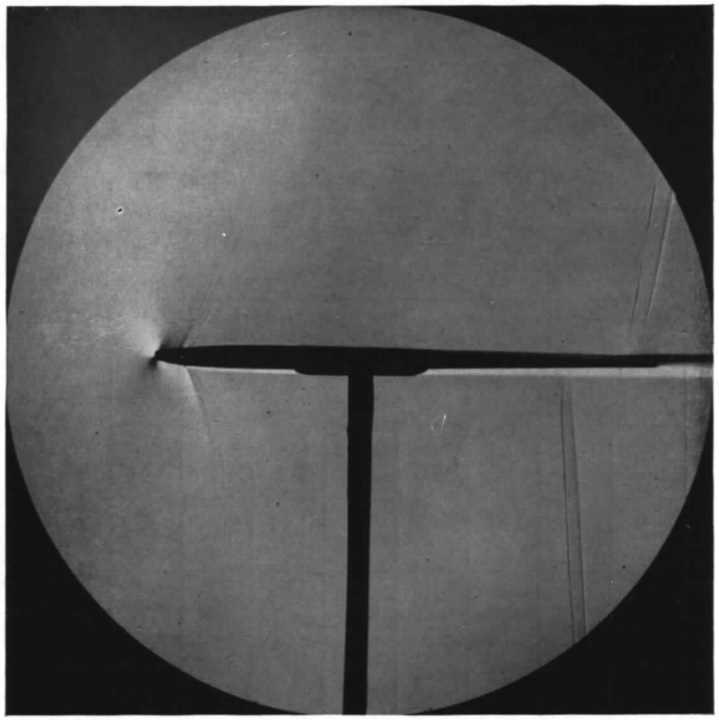

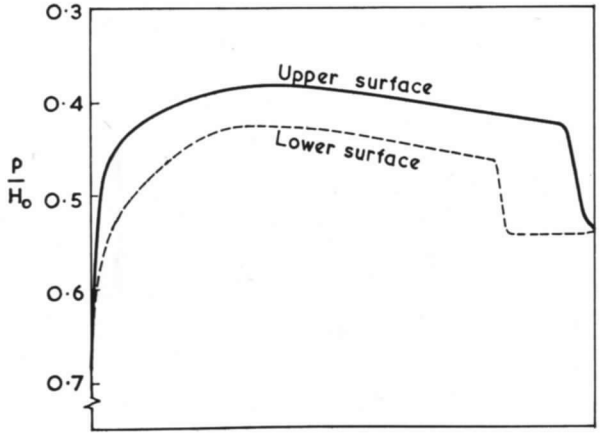

FIG. 49. The flow at $M_0 = 1{\cdot}010$, $\alpha = 1$ deg.

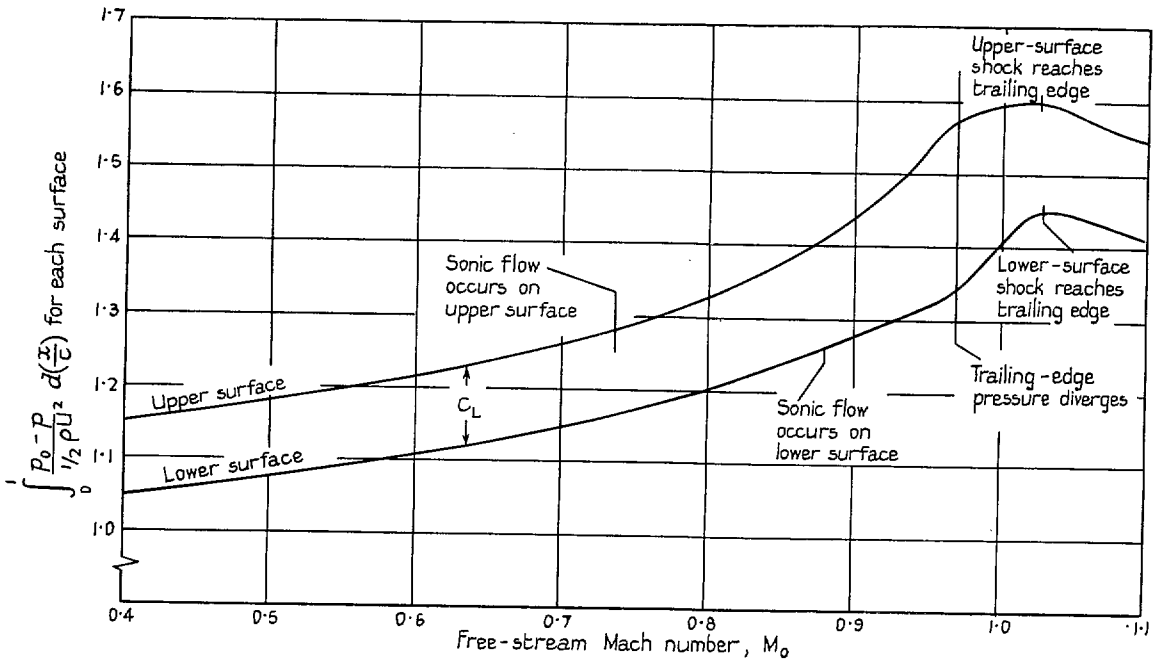

FIG. 50. Contributions of the upper and lower surfaces to C_L at $\alpha = 1$ deg.

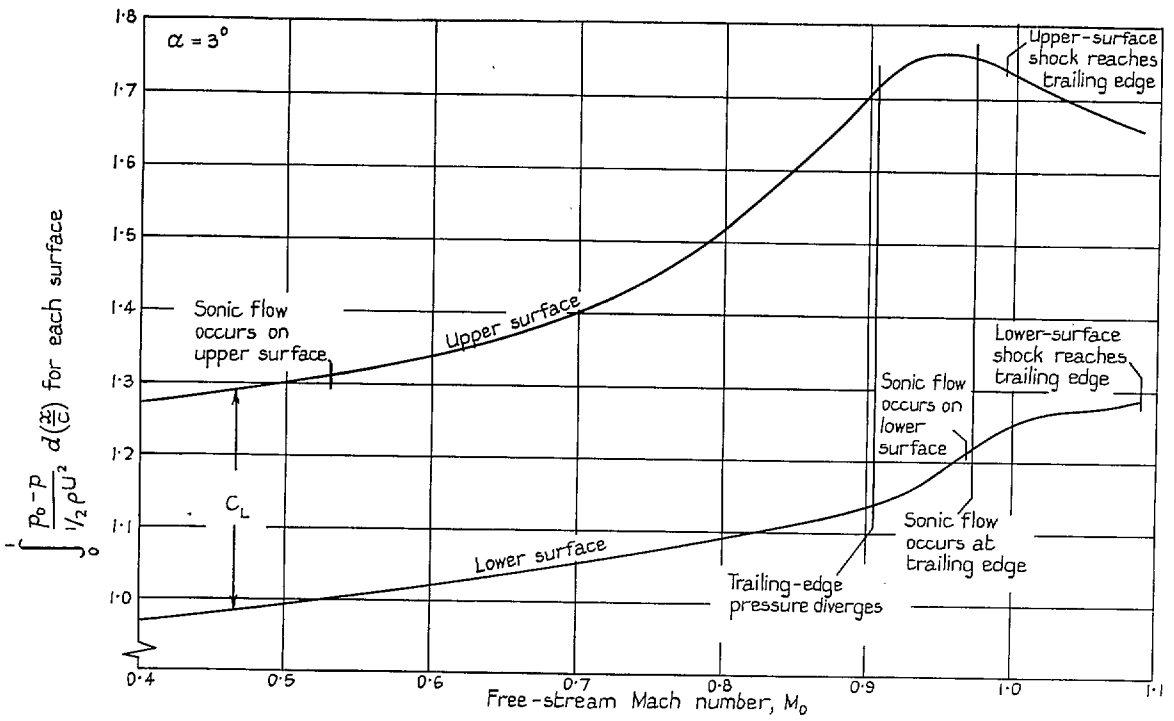

FIG. 51. Contributions of the upper and lower surfaces to C_L at $\alpha = 3$ deg.

(73940) Wt. 53/2293 K.7 11/58 Hw.

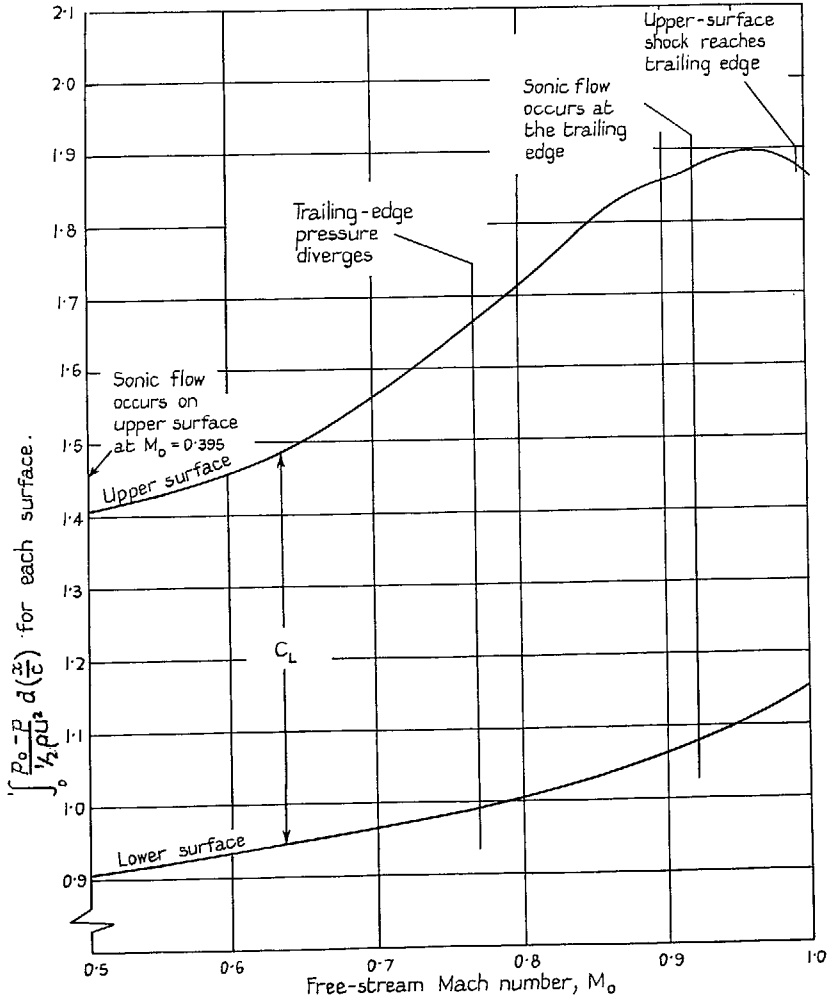

FIG. 52. Contributions of the upper and lower surfaces to C_L at $\alpha = 5$ deg.

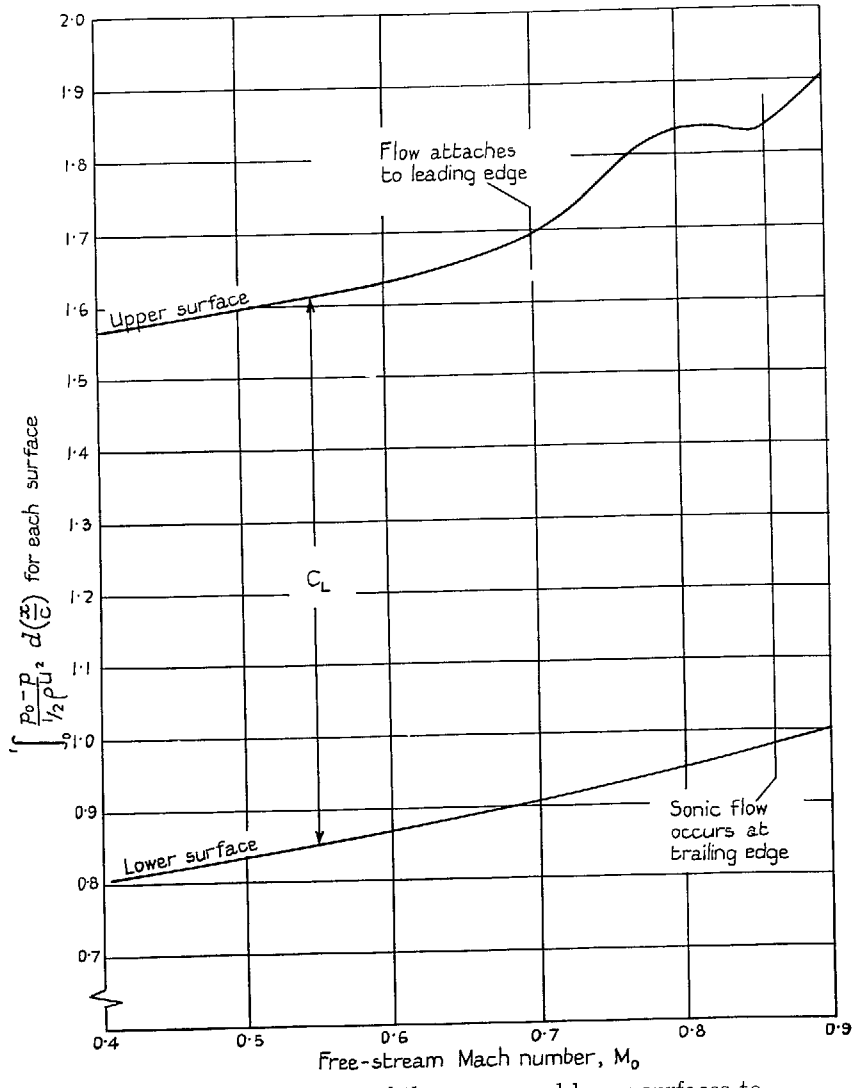

FIG 53. Contributions of the upper and lower surfaces to C_L at $\alpha = 8$ deg.

PRINTED IN GREAT BRITAIN

Publications of the Aeronautical Research Council

ANNUAL TECHNICAL REPORTS OF THE AERONAUTICAL RESEARCH COUNCIL (BOUND VOLUMES)

1939 Vol. I. Aerodynamics General, Performance, Airscrews, Engines. 50*s.* (52*s.*).
Vol. II. Stability and Control, Flutter and Vibration, Instruments, Structures, Seaplanes, etc. 63*s.* (65*s.*)

1940 Aero and Hydrodynamics, Aerofoils, Airscrews, Engines, Flutter, Icing, Stability and Control, Structures, and a miscellaneous section. 50*s.* (52*s.*)

1941 Aero and Hydrodynamics, Aerofoils, Airscrews, Engines, Flutter, Stability and Control, Structures. 63*s.* (65*s.*)

1942 Vol. I. Aero and Hydrodynamics, Aerofoils, Airscrews, Engines. 75*s.* (77*s.*)
Vol. II. Noise, Parachutes, Stability and Control, Structures, Vibration, Wind Tunnels. 47*s.* 6*d.* (49*s.* 6*d.*)

1943 Vol. I. Aerodynamics, Aerofoils, Airscrews. 80*s.* (82*s.*)
Vol. II. Engines, Flutter, Materials, Parachutes, Performance, Stability and Control, Structures. 90*s.* (92*s.* 9*d.*)

1944 Vol. I. Aero and Hydrodynamics, Aerofoils, Aircraft, Airscrews, Controls. 84*s.* (86*s.* 6*d.*)
Vol. II. Flutter and Vibration, Materials, Miscellaneous, Navigation, Parachutes, Performance, Plates and Panels, Stability, Structures, Test Equipment, Wind Tunnels. 84*s.* (86*s.* 6*d.*)

1945 Vol. I. Aero and Hydrodynamics, Aerofoils. 130*s.* (132*s.* 9*d.*)
Vol. II. Aircraft, Airscrews, Controls. 130*s.* (132*s.* 9*d.*)
Vol. III. Flutter and Vibration, Instruments, Miscellaneous, Parachutes, Plates and Panels, Propulsion. 130*s.* (132*s.* 6*d.*)
Vol. IV. Stability, Structures, Wind Tunnels, Wind Tunnel Technique. 130*s.* (132*s.* 6*d.*)

Annual Reports of the Aeronautical Research Council—

1937 2*s.* (2*s.* 2*d.*) 1938 1*s.* 6*d.* (1*s.* 8*d.*) 1939–48 3*s.* (3*s.* 5*d.*)

Index to all Reports and Memoranda published in the Annual Technical Reports, and separately—

April, 1950 - - - - R. & M. 2600 2*s.* 6*d.* (2*s.* 10*d.*)

Author Index to all Reports and Memoranda of the Aeronautical Research Council—

1909—January, 1954 R. & M. No. 2570 15*s.* (15*s.* 8*d.*)

Indexes to the Technical Reports of the Aeronautical Research Council—

December 1, 1936—June 30, 1939	R. & M. No. 1850	1*s.* 3*d.* (1*s.* 5*d.*)
July 1, 1939—June 30, 1945	R. & M. No. 1950	1*s.* (1*s.* 2*d.*)
July 1, 1945—June 30, 1946	R. & M. No. 2050	1*s.* (1*s.* 2*d.*)
July 1, 1946—December 31, 1946	R. & M. No. 2150	1*s.* 3*d.* (1*s.* 5*d.*)
January 1, 1947—June 30, 1947	R. & M. No. 2250	1*s.* 3*d.* (1*s.* 5*d.*)

Published Reports and Memoranda of the Aeronautical Research Council—

Between Nos. 2251–2349	R. & M. No. 2350	1*s.* 9*d.* (1*s.* 11*d.*)
Between Nos. 2351–2449	R. & M. No. 2450	2*s.* (2*s.* 2*d.*)
Between Nos. 2451–2549	R. & M. No. 2550	2*s.* 6*d.* (2*s.* 10*d.*)
Between Nos. 2551–2649	R. & M. No. 2650	2*s.* 6*d.* (2*s.* 10*d.*)
Between Nos. 2651–2749	R. & M. No. 2750	2*s.* 6*d.* (2*s.* 10*d.*)

Prices in brackets include postage

HER MAJESTY'S STATIONERY OFFICE

York House, Kingsway, London W.C.2; 423 Oxford Street, London W.1; 13a Castle Street, Edinburgh 2; 39 King Street, Manchester 2; 2 Edmund Street, Birmingham 3; 109 St. Mary Street, Cardiff; Tower Lane, Bristol 1; 80 Chichester Street, Belfast, *or through any bookseller.*

S.O. Code No. 23-3109